Meteorol Atmos Phys (2018) 130:701–724
https://doi.org/10.1007/s00703-017-0540-y

ORIGINAL PAPER

Analysis of temperature data over semi-arid Botswana: trends and break points

Kgakgamatso Mphale[1] · Akintayo Adedoyin[1] · Godiraone Nkoni[1] · Galebonwe Ramaphane[1] · Modise Wiston[1] · Oyapo Chimidza[1]

Received: 16 August 2016 / Accepted: 14 June 2017 / Published online: 26 June 2017

Abstract Climate change is a global challenge which impacts negatively on sustainable rural livelihoods, public health and economic development, more especially for communities in Southern Africa. Assessment of indices that signify climate change can inform formulation of relevant adaptation strategies and policies for the communities. Diurnal temperature range (DTR) is acknowledged as an expedient measure of the scourge as it is sensitive to variations in radiative energy balance. In this study, a long-term (1961–2010) daily temperature data obtained from nine (9) synoptic stations in Botswana were analyzed for monotonic trends and epochal changes in annual maximum (T_{max}), minimum (T_{min}) temperatures and DTR time series. Most of the considered stations were along the Kalahari Transect, a region which is at high risk of extensive environmental change due to climate change. Mann–Kendall trend and Lepage tests were applied for trend and change point analysis, respectively. The statistical analysis shows that stations in the southern part of the country experienced significant negative trends in annual DTR at the rate of −0.09 to −0.30 °C per decade due to steeper warming rates in annual T_{min} than annual T_{max} trends. On the contrary, stations in the northern part of the country experienced positive trends in annual DTR brought about by either a decreasing annual T_{min} trend which outstripped annual T_{max} or annual T_{max} which outpaced annual T_{min}. The increasing trends in DTR varied from 0.25 to 0.67 °C per decade. For most of the stations, the most significant annual DTR trends change point was in 1982 which coincided with the reversal of atmospheric circulation patterns.

Responsible Editor: A. P. Dimri.

✉ Kgakgamatso Mphale
mphalekm@mopipi.ub.bw

[1] Physics Department, University of Botswana, P/Bag 0022, Gaborone, Botswana

1 Introduction

Anthropogenic greenhouse gas emissions from fossil fuel combustion and other sources (e.g., forest fires) to the atmosphere have increased by about 49% since 1990 and their yearly emission rate had been accelerated to 5.9% in 2010 (McMichael et al. 2012). The increase in the amount of greenhouse gases in the atmosphere has intensified greenhouse effect and consequently led to global warming (Freiwan and Kadioğlu 2008). Numerous studies have revealed that global mean surface air temperature has increased by 0.3–6.0 °C over the last century (Türkeş et al. 1996; King'uyu et al. 2000; Bisai et al. 2014). The fifth Assessment Report (AR5) of the Intergovernmental Panel on Climate Change (IPCC) also shows that global air temperature has continued to rise at rate of 0.08–0.14 °C per decade since 1951 (IPCC 2013).

Global circulation models (GCMs) forced with emission scenarios from the IPCC's Special Report on Emission Scenarios (SRES) predict that by the end of twenty-first century, global average temperature will rise by about 1.1–6.4 °C relative to the 1980–1999 average (Meehl et al. 2007). At regional scale, regional climate models (RCMs) have also been employed to simulate the effects of continued current emission rate of greenhouse gases into the atmosphere on future climate of Southern Africa (e.g., Tadross et al. 2005; Davis 2011). From the numerical experiments, it is anticipated that Southern Africa will be

hotter and drier by the end of the century. Its mean surface air temperature is projected to be 3–4 °C warmer by the 2080s.

The change in global and regional climate is anticipated to deleteriously affect sustainable rural livelihoods, public health, natural resources and economic development of communities in Southern Africa. Rockström (2000) notes that communities in this region are vulnerable to the scourge as they are very much contingent on resources that are sensitive to environmental change, e.g., rain-fed agriculture. Changes in temperature regime may, through its association with plant's transpiration and stomatal functioning, upset nutrient balance in arable crops which is necessary for better growth and high-quality yields (Inthichack et al. 2013). They may also promote the emergence of new livestock macro-parasites (Moreki and Tsopito 2013). It is noteworthy that about 60% of Southern Africa's population lives below poverty datum line and has low adaptive capacity. Urquhart (2008) and Mavhura et al. (2015) note that besides poverty, inadequacies in environmental and climate change governance are some of the factors that contribute to the region's low adaptive capacity.

Botswana is a semi-arid country in sub-Saharan Africa with an economy that is dependent on subsistence agro-pastoralism and natural resources. The sectors are sensitive to changes in daily temperature and are under threat from rangeland degradation, desertification, biodiversity loss and climate change. According to Food and Agricultural Organization (FAO) working paper on forests, rangelands and climate change in Southern Africa, the country lacks national climate change policy and strategy which could facilitate implementation of its climate change action plan (Naidoo et al. 2013). In light of the emergent environmental and socio-economic stressors, studies on climate change are very important as they can inform the policy formulation.

Although long-term changes in mean temperature and other hydro-meteorological variables have been used as indicators of climate change (e.g., in Unganai 1996; Toreti and Desaito 2007; Shahid and Hazarika 2010; Tabari et al. 2012; Boretti 2013; Borges et al. 2014), an informative and useful index for detecting the global phenomenon is diurnal temperature range (Shahid et al. 2012; Manatsa et al. 2015). The diurnal temperature range (DTR) is the difference between daily maximum (T_{max}) and minimum (T_{min}) temperatures. The variable is sensitive to variations in radiative energy balance and it is therefore an expedient measure of climate change. Besides, the impacts of the scourge are felt more strongly through temperature extremes (Wang et al. 2014; Manatsa et al. 2015).

Consequently, trends in annual T_{min}, T_{max} and DTR have been analyzed on regional and global scale (e.g., in Türkeş et al. 1996; Easterling et al. 1997; Brunetti et al. 2000; Kruger and Shongwe 2004; del Rio et al. 2007; Zhou et al. 2009; Tabari et al. 2011; Manatsa et al. 2015). The studies reveal that there are spatial and temporal variability in DTR, with some regions showing divergent trends in the thermometric variable. The regional inconsistencies in the trends are attributable to cloud cover, land surface biophysical properties and atmospheric circulation (Brunetti et al. 2000). Research also reveals that semi-arid and arid lands experienced the most significant decreasing trends in the DTR since the 1950s (Zhou et al. 2007).

Van Regenmortel (1995) has analyzed annual and seasonal T_{max} and T_{min} for Botswana over a 25-year period (1960–1984) and reported a positive trend in both the temperature indices. The analysis also revealed that the most significant trend was that of mean T_{max} during winter with a warming of about 0.32 °C per decade. Hitherto, there is very little or no comprehensive recent study carried out on long-term trend analysis of T_{min}, T_{max} and DTR in Botswana. Nonetheless, New et al. (2006) studied daily climate extremes over Southern Africa from 1961 to 2000. The analysis showed that there is an increasing trend in DTR in a zone across Botswana and other central southern African countries associated with steeper trends in T_{max} than T_{min} indices. Because of the regional scope of the study, ecologically fragile regions such as the Kalahari Transect were inadequately covered. In a related study, simulations using SCENGEN, a coupled gas cycle–climate model, suggest that DTRs in Botswana are likely to range from −0.3 to 0.0 °C by the end of 2037 (Moreki and Tsopito 2013).

The objective of the study is to explore the existence of significant long-term monotonic trends and change points in mean annual T_{min}, T_{max} and DTR time series using recent records for the country as they provide useful information on climate change and variability. The long-term temperature time series analysis provides an opportunity to access the potential sustainability of agro-pastoral systems in the country that are heavily affected by climate variability. Moreover, the precise causes of changes in T_{min}, T_{max} and DTR together with their regional and seasonal variation remain poorly understood. As in other tropical countries, the temperature extremes have a potential to impact on public health by promoting waterborne diseases. Therefore, the analysis will inform the development of effective mitigation and adaptive strategies designed to protect vulnerable communities in the country.

In the manuscript, Sect. 2 describes the study area and data sets used. Simple linear regression method has been employed to determine the trends in T_{min}, T_{max} and DTR. The significance of the trends is determined by a non-parametric Mann–Kendall test. The statistical procedures used in the analysis are described in Sect. 3. Methods of

identification of change point years in the time series are also discussed in the section. Section 4 presents and discusses the results of the analysis. The manuscript is concluded in Sect. 5 with future direction of the investigation.

2 Study area and data availability

2.1 Study area

Botswana is land-locked country in the center of the great southern African Plateau. It is situated between the 18°S and 27°S latitudes and 20°E and 29°E longitudes (Fig. 1). The sub-Saharan African country has an average altitude of 1000 m above sea level and landmass of 582,000 km^2. It can be categorized into two major ecological regions: the sand and hard veldt. The largest of the eco-regions is the sand veldt which covers about 80% of the land mass. The region stretches along the western part of the country and forms part of the vast Kalahari sand sheet. The ecoregion is characterized by arenosol soils which are 100–200 m deep. The soils are generally infertile and free-draining because of low organic matter content. To the eastern part of the country lies the hard veldt, an ecological region which is characterized by highly leached ferruginous tropical soils (Darkoh 1999).

The country is situated under the descending limb of the Hadley cell circulation and consequently has arid to semi-arid climate (Batisani and Yarnal 2010). Its summers are generally warm and wet while winters are cold and dry. The country's rainfall is unimodal and above 80% of it occurs between October and April. It varies from an average maximum of over 650 mm in the north east to average minimum of 250 mm in the south west region (Darkoh 1999). The rainfall is erratic and unevenly distributed throughout the country. As for the temperatures, average maximum temperature for the hottest month (December) is about 35 °C while mean minimum temperatures of about 3 °C and occurs in July (Mogotsi et al. 2011). Chipanshi et al. (2003) note that mean annual potential evapotranspiration rate is generally very much higher than mean annual precipitation as it is over 1000 mm per annum.

About 40% of Botswana's 2.2 million population lives on rural fragile land. More than half of the rural community is poverty stricken (Malema 2012). The population relies primarily on arable agriculture and other natural resources for its source of food and income (Legwaila et al. 2011). According to Nfila and Jain (2011), the country is critically dependent on its natural resources as approximately 75% of paid employment can be linked to natural resources. Poor infertile soils and erratic rainfall has led to less than 5% of the country being suitable for rain-fed agriculture. The suitable regions are predominantly in the hard veldt. The sand veldt region is predominantly a beef production area because of its paucity of surface water.

Climate change makes the country highly vulnerable to environmental and socio-economic problems. Rangeland degradation and desertification are major environmental problems facing the country particularly in the south western region (Reed et al. 2015; Dougill et al. 2016). The reason is partly due to the fact that many of its inhabitants practice subsistence farming on varying scales and at varying intensities (Stringer et al. 2009). Overstocking of domesticated grazing animals in this region has led to overgrazing of vegetation and subsequently land degradation. There is also an increase of human activity expansion into the region, with about 70% of dry areas being turned into agro-pastoral systems (Madzwamuse et al. 2007).

2.2 Data sources

Monthly maximum and minimum temperature data used in the study were obtained from nine (9) of the seventeen (17) synoptic stations which are operated by Department of Meteorological Services (DMS) of Botswana. The stations, shown in Fig. 1, were selected on the basis of the fact that they are fairly well distributed throughout the study area and have at least a 30-year-long data. Three (3) of the selected stations (i.e., Gaborone, Mahalapye and Francistown) are in the hard veldt while the rest are in the sand veldt region. The number of stations considered in sand veldt is greater than those from the hard veldt so as to address the issue of paucity of information on daily temperature trends in the region.

The station data were collected to the standards of World Meteorological Organization (WMO) and stored in a database at DMS. Most of the data were about 50 years long except for Kasane (Table 1). The longest dataset was 53 years long (from 1st January 1961 to 31st December 2013). Quality control procedure to identify and correct outliers in the dataset was carried out as described in Mphale et al. (2014). Missing data were less than 2% of the whole dataset and was interpolated with the help of linear regression method to fill the gaps, e.g., in Liu et al. (2006). Thenceforth, the data were tested for homogeneity using the Thom test. Inhomogeneity due to station relocation was detected for some stations, e.g., Gaborone. A method suggested by Gajić-Čapka and Zaninović (1997) was employed to correct the non-homogeneity in the data sets.

The time-series data were subdivided into meteorological seasons: summer defined as from December to February, autumn from March to May, winter from June to August and spring from September to November. The data were averaged to get annual and seasonal values for each station according to the standards of the DMS.

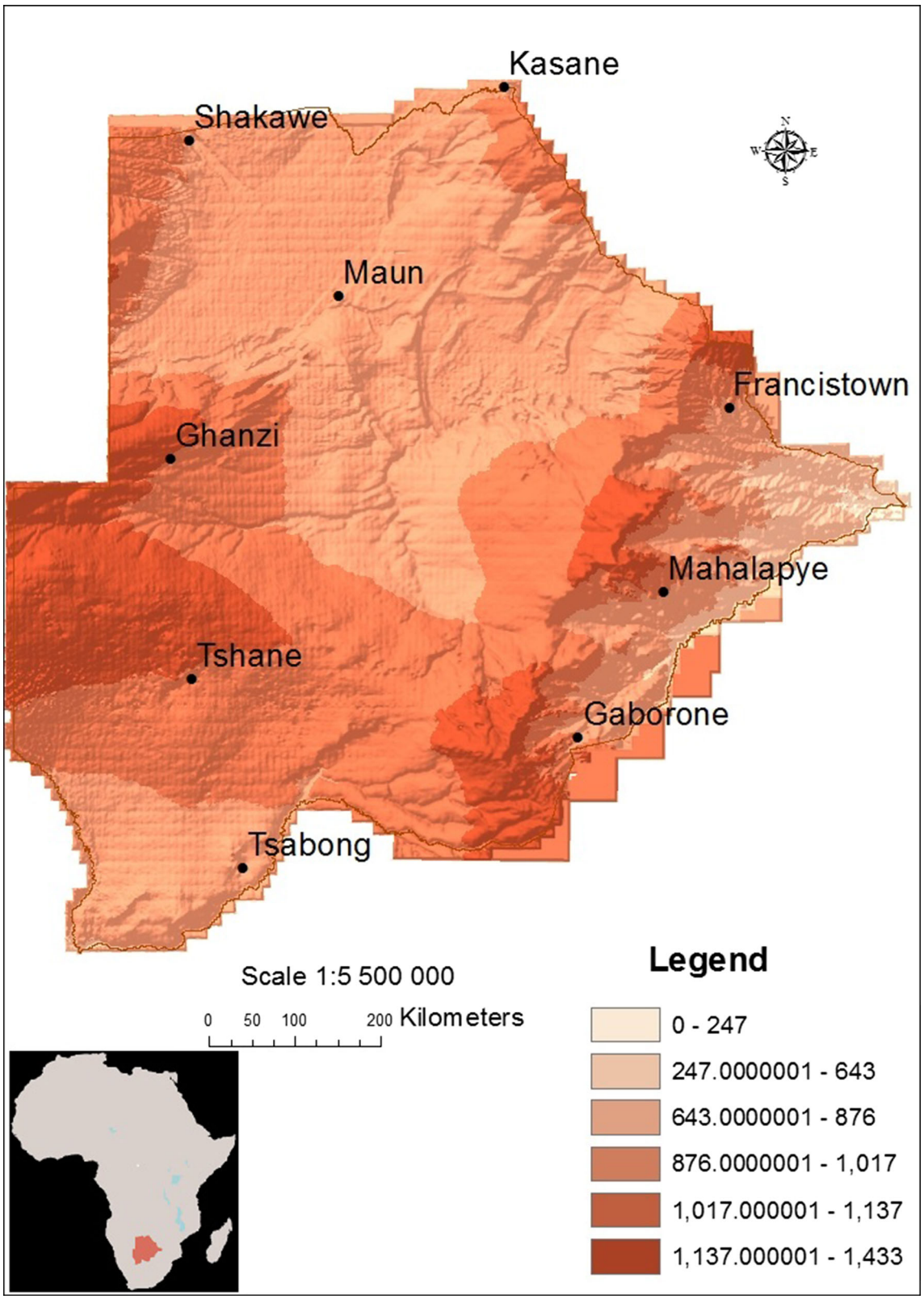

Fig. 1 Location of the study area and distribution of synoptic stations

Table 1 Geographical locations, elevations and length data for synoptic stations considered in the study

Station	Lat (°S)	Long (°E)	Elev (m.a.sl.)	Period of record
(1) Francistown (68054)	21.17	27.48	1001	1961–2013
(2) Gaborone(68244)	24.65	25.91	1010	1961–2013
(3) Ghanzi (68024)	24.40	25.55	1131	1962–2013
(4) Kasane (68029)	17.82	25.17	968	1984–2013
(5) Mahalapye (68148)	23.07	26.83	1006	1963–2013
(6) Maun (68032)	19.98	23.42	945	1966–2013
(7) Shakawe (68026)	18.37	21.85	1032	1966–2013
(8) Tsabong (68328)	26.05	22.45	960	1962–2013
(9) Tshane (68226)	24.02	21.88	1118	1962–2013

Cloud cover monthly data were obtained from University of East Anglia's Climate Research Unit (CRU) time series (TS) version 3.22 dataset which spans from 1901 to 2013. The data are freely available from the website: http://badc.nerc.ac.uk/browse/badc/cru/data. It is a product of an extrapolation calculated on high resolution (0.5° × 0.5°) grids from observations made at more 4000 National Meteorological Services station distributed around the world.

Data on atmospheric circulation, e.g., specific humidity, horizontal and vertical wind vectors, were obtained from National Oceanic and Atmospheric Administration's Earth System Research Laboratory (NOAA-ESRL), Colorado, USA. The website for downloading the data is: http://www.esrl.noaa.gov/psd/data/gridded/data.ncep.reanalysis.html. The reanalysis data starts from 1948 to present. The NCEP–NCAR reanalysis data have a horizontal resolution of 2.5° × 2.5° (Kalnay et al. 1996).

3 Methodology

3.1 Test for homogeneity

A homogeneous climatological time series is that in which variations are due to climatic and weather events. It is therefore imperative that climate data which contain changes which are not weather or climate related be adjusted. Several methods have been developed for analysis of inhomogeneity in time series, e.g., cumulative deviations procedure (Buishand 1982), von Neumann test (von Neumann 1941), Bayesian procedure (Chernoff and Zacks 1964), just to name a few. A popular homogeneity test method which is recommended by WMO and has been used by numerous researchers is Run or Thom test.

The Thom test is a non-parametric statistical procedure which has been used for absolute homogeneity analysis of seasonal and annual rainfall time series (e.g., in Rodrigo et al. 1999; Modarres and Silva 2007). Nasri and Modarres (2009) have used the test to assess heterogeneity in annual maximum dry spell length and annual number of dry spell period data. When analyzing trend in growing degree-days in Turkey, Kadioğlu and Şaylan (2001) used the statistical procedure to evaluate heterogeneity in temperature time series. Besides being robust against possible outliers, its test statistic is easy to compute and implement. In the study, the Thom test was employed to determine homogeneity in the annual $T_{\min}$ and $T_{\max}$ time series in the following manner:

The annual $T_{\min}$ and $T_{\max}$ time series were arranged in the order in which they were recorded at the synoptic stations, i.e., in the order:

$$x_i = \{x_1, x_2, x_3, \ldots, x_n\}. \quad (1)$$

The median value of each time-series data, x_{med}, was calculated. The data were then ranked in such a way that if a datum (x_i) was below the median, i.e., ($x_i < x_{\text{med}}$), a code 'L' was assigned to it and contrariwise, a code 'H' was assigned. Thus, we got an uninterrupted and interrupted sequence of Ls and Hs called Runs (R). The number of R was then determined. If the total number of data points (n) is large, i.e., $n \geq 25$, the distribution function of number of the runs becomes Gaussian with average (E) and variance (Var) given by the following relations (Rodrigo et al. 1999):

$$E(R) = \frac{(n+2)}{2} \quad (2)$$

and

$$\text{Var}(R) = \frac{n(n-2)}{4(n-1)}. \quad (3)$$

The statistic for determining if the time-series data is homogeneous or not is given by the expression:

$$Z_t = \frac{R - E(R)}{\sqrt{\text{Var}(R)}}. \quad (4)$$

If $|Z_t| \leq 2.58$, then the time-series data are homogeneous at 99% confidence level.

3.2 Normality test

Normality in the temperature data was investigated by applying standardized skewness and kurtosis test. This is a

common procedure which was applied by several researchers as it is time-saving and simple (Brazel and Balling 1986; Mphale et al. 2014). If the absolute values of the skewness and kurtosis coefficients are greater than 1.96, then it implies that the distribution function of the data has significantly deviated from Gaussian distribution at 95% confidence level.

3.3 Randomness test

One major problem which affects evaluation and detection of trends in hydro-meteorological time series is autocorrelation (Partal and Kahya 2006; Tabari and Talaee 2011). Nasri and Modarres (2009) note that the existence of significant positive autocorrelation coefficient in time series increases chances of erroneous probabilities in trend analysis. Thus, an application of a non-parametric trend test will suggest existence of significant trend when in fact it does not exist. Therefore, data must be assessed for serial independence before monotonic trend evaluation is carried out. An autocorrelation function used to check randomness or independence in time series is given by Von Storch (1995) as:

$$r_k = \frac{\sum_{i=1}^{n-k}(x_i - m)(x_{i+k} - m)}{\sum_{i=1}^{n}(x_i - m)^2}, \quad (5)$$

where r_k is the lag-k autocorrelation coefficient; m is mean value of the time series; n and k are the number of observations and time lag, respectively.

The autocorrelation coefficients should be close to zero and should not exceed the confidence interval at any desired significance level. At any significance level, confidence intervals are determined from the relation (Nasri and Modarres 2009):

$$\mathrm{CI} = \frac{(z_\alpha - \alpha/2)}{\sqrt{n}}, \quad (6)$$

where α is significance level, and z is percent point function of the normal distribution.

To eliminate the influence of autocorrelation in trend analysis, data must be 'pre-whitened' (Douglas et al. 2000). A powerful pre-whitening procedure which has been used by several researchers is the trend-free pre-whitening (TFPW), e.g., in Yue et al. (2002), Tabari et al. (2012) and Blain (2013). The procedure is as follows:

(i) Consider annual $T_{\min}$ and $T_{\max}$ time series (x_i) given by the following relation:

$$x_i = \{x_1, x_2, x_3, \ldots, x_n\}. \quad (7)$$

(ii) A de-trended time series (Y_i) is first obtained from the original time series (x_i) as:

$$Y_i = x_i - (\beta \times i), \quad (8)$$

where β is the Theil–Sen estimator. The estimator is calculated by the following expression:

$$\beta = \text{median}\left[\frac{(x_j - x_i)}{(j-1)}\right], \quad \text{for all } i < j. \quad (9)$$

(iii) Obtain the residual data through the following operation:

$$Y_i' = Y_i - r_1 \times Y_{i-1}, \quad (10)$$

where r_1 the lag-1 correlation obtained from Eq. (5).

(iv) Then value $(\beta \times i)$ is then added to residual data to obtain the final "pre-whitened" time series (Y_i'') given by:

$$Y_i'' = Y_i' - (\beta \times i). \quad (11)$$

3.4 Trend analysis

3.4.1 Simple linear regression

Simple linear regression is a parametric method which is commonly used to determine the presence of monotonic trend in hydro-meteorological time series (e.g., in Borges et al. 2014; Knežević et al. 2014; Zarenistanak et al. 2015). It describes the relation of one variable (y_i) with another of interest (x_i). The method allows one to obtain trend or slope (b) of a hydro-meteorological variable with time from the following regression equation:

$$y_i = a + b \times x_i + e, \quad (12)$$

where a and e are intercept and random error, respectively. The slope can be determined from the relation (Borges et al. 2014):

$$b = \frac{\frac{12}{n}\left\{\sum_{i=1}^{N}(t_i \times y_i) - \frac{n+1}{2}\sum_{i=1}^{n} y_i\right\}}{n^2 - 1}. \quad (13)$$

Positive values of the slope give increasing trend while negative ones signify a decreasing trend.

3.4.2 Mann–Kendall trend test

The existence of significant trends in hydro-meteorological time series is usually evaluated using Mann–Kendall (MK) test (Douglas et al. 2000; Kadioğlu and Şaylan 2001; Modaraes and Silva 2007; Saboohi et al. 2012; Knežević et al. 2014; Borges et al. 2014). MK is a non-parametric rank-based test which is distribution free and is known to be resistant to effects of outliers (Kadioğlu and Şaylan 2001; Nasri and Modarres 2009). To detect significant trends in the temperature time series, we proceeded as follows.

Consider an ordered time series of variable $x_i = \{x_1, x_2, x_3, \ldots, x_n\}$ with length n. Each datum (x_i) in the series is compared with the subsequent one (x_j). If the time series has insignificant lag-1 autocorrelation coefficient, then Mann–Kendall statistic (S) can be described as:

$$S = \sum_{i=1}^{n-1} \sum_{j=i+1}^{n} \text{sign}(x_j - x_i), \tag{14}$$

where x_i and x_j are sequential data for the ith and jth terms, respectively, and

$$\text{sign}(x_i - x_j) = \begin{cases} 1 & \text{if } (x_i - x_j) > 0 \\ 0 & \text{if } (x_i - x_j) = 0 \\ -1 & \text{if } (x_i - x_j) < 0 \end{cases}. \tag{15}$$

The statistic S is approximately Gaussian when $n \geq 18$ with the mean $E(S)$ and variance Var(S) of the statistic S given by the following expressions:

$$E(S) = 0 \tag{16}$$

and

$$\text{Var}(S) = \frac{n(n-1)(2n+5)}{18}. \tag{17}$$

However, if ties exist in the time series, then the expression for Var(S) has to be adjusted and becomes:

$$\text{Var}(S) = \frac{\left\{n(n-1)(2n+5) - \sum_{p=1}^{q} t_p(t_p-1)(2t_p+5)\right\}}{18}. \tag{18}$$

The variable q and t_p in Eq. (18) are number of tied groups and number of data values in the pth group, respectively. The standardized statistic (Z_{mk}) for one-tailed test of the statistic S is given as follows:

$$Z_{\text{mk}} = \begin{cases} \dfrac{S-1}{\sqrt{\text{Var}(S)}} & \text{if } S > 0 \\ 0 & \text{if } S = 0 \\ \dfrac{S-1}{\sqrt{\text{Var}(S)}} & \text{if } S < 0 \end{cases}. \tag{19}$$

If Z_{mk} is positive then the trend is increasing, and if Z_{mk} is negative then the trend is decreasing. At 95% confidence level the null hypothesis of no trend is rejected if $|Z_{\text{mk}}| \geq 1.96$, and it is also rejected at 99% confidence level if $|Z_{\text{mk}}| \geq 2.575$.

3.5 Change point detection

Several non-parametric statistical methods have been applied by many researchers to identify change points in climatological time-series data, e.g., in Moraes et al. (1998), Safari (2012), Ye et al. (2013), Yao and Li (2014). In the study, non-parametric Lepage test was used to detect change points in the annual T_{min} and T_{max} time series. According to a review by Rodionov (2005), the test is more powerful than other similar non-parametric tests, such the Student's t test, and Wilcoxon–Mann–Whitney test. Furthermore, numerous researchers have employed the Lepage test to study abrupt changes in precipitation, temperature and other hydro-meteorological variables time-series, e.g., Yonetani (1993), Vivès and Jones (2005) and Liu et al. (2011). However, the test is limited in that it is poor in detecting step-like changes when the sample size (n) is large and its optimal n is 10 (Vivès and Jones 2005). To complement the Lepage test, an effective non-parametric sequential Mann–Kendall rank (SQMK) test was used. Besides being simple to calculate, the SQMK is insensitive to a small number of outliers which might be in a time-series data and can be used for detection of several change points in the series (Chatterjee et al. 2014).

3.5.1 Lepage test

Lepage test, a combination of Wilcoxon and Ansari–Bradley statistics, is a two-sample test for location and dispersion which follows the Chi-square (χ^2) distribution with two degrees of freedom. Its test statistic (HK) is given as (Yang et al. 2009):

$$\text{HK} = \frac{[W - E(W)]^2}{V(W)} + \frac{[A - E(A)]^2}{V(A)}, \tag{20}$$

where $W = \sum_{i=1}^{n_1+n_2} iu_i$, (21)

$$A = \sum_{i=1}^{n_1+n_2} iu_i + \sum_{i=n_1+1}^{n_1+n_2} (n_1 + n_2 - i + 1)u_i, \tag{22}$$

$$E(W) = \frac{n_1(n_1+n_2+1)}{2} \tag{23}$$

and

$$\text{Var}(W) = \frac{n_1 n_2 (n_1+n_2+1)}{12}. \tag{24}$$

If $n_1 + n_2$ is even, then:

$$E(A) = \frac{n_1(n_1+n_2+2)}{4} \tag{25}$$

and

$$\text{Var}(A) = \frac{n_1 n_2 (n_1+n_2+2)(n_1+n_2-2)}{48(n_1+n_2-1)}. \tag{26}$$

Else if $n_1 + n_2$ is odd, then

$$E(A) = \frac{n_1(n_1 + n_2 + 1)^2}{4(n_1 + n_2)} \quad (27)$$

and

$$\mathrm{Var}(A) = \frac{n_1 n_2 (n_1 + n_2 + 1)\{(n_1 + n_2)^2 + 3\}}{48(n_1 + n_2)^2}. \quad (28)$$

In the study, the Lepage test was applied in the following manner: consider a year Y in the annual $T_{\min}$ or $T_{\max}$ time series. Two independent samples $x_i = \{x_1, x_2, x_3, \ldots, x_{n_1}\}$ and $y_i = \{y_1, y_2, y_3, \ldots, y_{n_2}\}$ were taken n_1 years before the year Y and n_2 years after, with the year Y inclusive, respectively. The sample size of 10 was used for both n_1 and n_2. The samples, x_i and y_i, were then re-combined and then ranked in an increasing order. For the ith observation of the ranked data, u_1 was set to 1 if it was from sample x_i or else was set to 0. The sequential HK statistic was then calculated using Eq. (20) starting with the year Y.

3.5.2 Sequential Mann–Kendall test

The sequential version of Mann–Kendall rank test (SQMK) is used to detect and locate an approximate starting point of a trend (Modarres and Sarhadi 2009). The test was successfully employed by several researchers to determine the existence of change points in climatological time-series data, e.g., in Moraes et al. (1998) and Bisai et al. (2014). The procedure for carrying out the analysis is as follows.

Consider time-series data x_i of length n, i.e., $(1 \leq i \leq n)$. The magnitudes of ranked values x_i are compared with x_j, where $j = (1, 2, 3, \ldots, i-1)$. At each comparison, number of cases for which $x_i > x_j$ is counted and denoted m_i.

The sum of m_i is given a statistic t_n such that:

$$t_n = \sum_{i=1}^{n} m_i. \quad (29)$$

For a large n, the population is normally distributed with mean ($E(t_n)$) and variance ($\mathrm{Var}(t_n)$) given by the following expressions:

$$E(t_n) = \frac{n(n-1)}{4} \quad (30)$$

and

$$\mathrm{Var}(t_n) = \frac{n(n-1)(2n+5)}{72}. \quad (31)$$

The SQMK test statistic, $u(t_n)$, is calculated from the relation:

$$u(t_n) = \frac{(t_n - E(t_n))}{\sqrt{\mathrm{Var}(t_n)}}. \quad (32)$$

The SQMK has Gaussian normal distribution with a zero mean and a unit standard deviation. Its sequential behavior fluctuates around zero level. In a similar way, a retrograde statistic $u'(t_n)$ is computed backwards starting from the end of the time series. The intersection of the curves $u(t_n)$ and $u'(t_n)$ localizes the beginning of the change. The starting point is significant at 95% confidence level if $|u(t_n)| \leq 1.96$.

4 Results and discussion

4.1 Mean values of annual $T_{\max}$ and $T_{\min}$

Mean annual $T_{\max}$ and $T_{\min}$ values for the each selected station are given in Table 2. It is observed from the table that stations in the northern part of the country (Kasane, Maun and Shakawe) were warmer than those in the south (Ghanzi, Mahalapye, Tsabong and Tshane) during the period of study. Kasane, Maun and Shakawe exhibited warmer mean annual $T_{\max}$ while Tsabong and Tshane were cooler in annual $T_{\min}$ than the rest of the

Table 2 Mean annual, Z statistics for Thom's test (Z_t), Z statistics for coefficients of skewness (Z_s) and kurtosis (Z_k) for $T_{\max}$ and $T_{\min}$ at the selected stations

Station	$T_{\max\_ave}$	$Z_{t_{\max}}$	$Z_{s\_t_{\max}}$	$Z_{k\_t_{\max}}$	$T_{\min\_ave}$	$Z_{t_{\min}}$	$Z_{s\_t_{\min}}$	$Z_{k\_t_{\min}}$
1. Francistown	28.7	−1.525	0.051	−0.298	13.4	−0.416	−0.263	−0.432
2. Gaborone	28.4	−0.149	0.050	−0.540	13.1	0.429	0.259	−0.723
3. Ghanzi	29.9	−0.295	−0.750	0.636	13.2	−1.010	0.158	−0.609
4. Kasane	30.4	−1.225	0.377	−0.298	15.8	−1.633	0.564	−0.583
5. Mahalapye	28.3	−1.250	−0.524	0.031	13.6	**−4.384**	0.002	−0.847
6. Maun	30.9	−1.789	−0.088	−0.074	15.6	**−3.579**	0.054	−0.521
7. Shakawe	30.5	−1.342	−0.434	−0.453	14.6	−2.082	−0.345	−0.176
8. Tsabong	29.3	−0.895	0.099	−0.096	11.3	**−2.918**	1.147	0.873
9. Tshane	29.2	0.000	−1.125	1.165	12.9	**−2.864**	−0.374	−0.027

Values in bold are not significant at 90% confidence level

stations. Stations at urban centers (Gaborone and Francistown) had the lowest mean annual T_{max}.

4.2 Homogeneity and normality analysis

Results of Thom test on time series are summarized in Table 2. The table also shows that for all the stations, annual T_{max} time series were homogeneous at 5% significance level as their absolute values for the Thom's test statistic ($Z_{t_{max}}$) were less than 1.96. It also depicts that the absolute values for annual T_{min} test statistic ($Z_{t_{min}}$) for the stations, Maun, Mahalapye, Tshane and Tsabong were above 2.58 (shown in italics and bold). This implied that the annual T_{min} data for the stations were not homogeneous and therefore needed adjustment. The largest deviation from homogeneity was in Mahalapye time series with $Z_{t_{min}}$ of −4.384.

Application of normality test on homogeneous annual T_{max} and T_{min} time series has shown that the series conformed to Gaussian distribution at 95% confidence level as the absolute values of the coefficients of skewness and kurtosis were all less than 1.96 (see Table 2). This implied that the parametric simple linear regression method could be used for trend analysis.

4.3 Autocorrelation

Figure 2 shows lag-1 autocorrelation coefficients of annual T_{max} time series for the stations. From the figure, it can be inferred that only Kasane had a negative lag-1 coefficient which was within the 95% confidence limit while the rest were positive. The figure also shows that coefficients for Francistown, Maun and Shakawe were not within the confidence limit (shown by dashed lines). Furthermore, it reveals that time series for Ghanzi and Tsabong had a strong serial independence as their coefficients are close to zero. When the same analysis was applied to annual T_{min} time series, positive lag-1 autocorrelation function coefficients which were significantly above the 95% confidence limit were obtained for almost all the stations (Fig. 2). Gaborone time series was the only one which did not show persistence. Taking note of the effects of auto-correlated time series on the null hypothesis of no trend in MK test, the time series with lag-1 autocorrelation coefficients which exceed the confidence limit were pre-whitened before trend analysis procedure was applied.

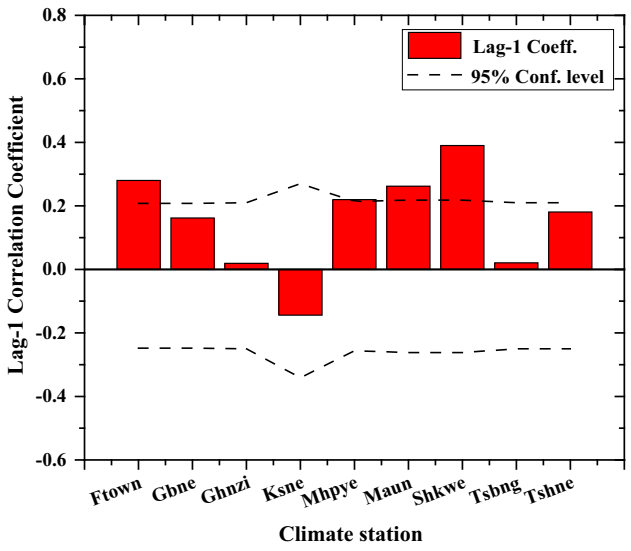

Fig. 2 Lag-1 autocorrelation coefficients for mean annual maximum temperatures at stations

4.4 Trend test

4.4.1 Annual T_{max} and T_{min} trends

Trend analysis results are summarized in Table 3. Application of both simple linear regression and MK test on the homogenized time series revealed that all stations except Gaborone and Kasane experienced significant positive trends (p value <0.1) in annual T_{max} during the period of study. Slopes from simple linear regression show that the significant positive trends varied from 0.14 to 0.45 °C per decade. Kasane experienced a significant cooling in annual T_{max} at the rate of −0.52 °C per decade. On the contrary, Gaborone was the only station which experienced insignificant cooling at rate of −0.07 °C per decade. The average trend for annual T_{max} for the country was observed to be 0.14 °C per decade. The observation is corroborated by findings from a trend analysis study conducted in the region by Kruger and Shongwe (2004). The researchers investigated temperature trends in South Africa over a 43-year-long (1960–2003) period and observed warming in T_{max} at the rate of 0.16 °C per decade. Still in Southern Africa, Unganai (1996) observed that the annual T_{max} for Zimbabwe increased by 0.10 °C per decade from 1933 to 1993. However, in a similar climatic environment (arid and semi-arid regions of Iran), Saboohi et al. (2012) observed steeper significant warming in annual T_{max} with an average of 0.2 °C per decade for the whole country.

Table 3 also shows that about 56% of the stations experienced significant warming in annual T_{min}. The significant positive trend ranged from 0.25 to 0.61 °C per decade at p values <0.01. Conversely, Shakawe and Kasane were the only stations noted to have experienced significant ($p < 0.01$) cooling at the rates of −0.18 and −0.87 °C per decade, respectively. Despite the significant trends, Gaborone and Francistown experienced insignificant warming in the order of 0.03 and 0.07 °C per decade, respectively. Average annual T_{min} trend for the country was observed to be 0.13 °C per decade. In a recent study on

Table 3 Trend slope and Mann–Kendall Z statistic (Z_{mk}) for T_{max} and T_{min} for the considered stations

Station	T_{max}			T_{min}		
	b (°C/10 years)	Z_{mk}	p valve	b (°C/10 years)	Z_{mk}	p value
1. Francistown	0.292	4.382	0.002	0.070	1.235	**0.136**
2. Gaborone	−0.070	−1.280	**0.132**	0.031	0.862	**0.166**
3. Ghanzi	0.144	2.504	0.042	0.251	4.512	0.001
4. Kasane	−0.516	−3.900	0.004	−0.866	−5.442	0.000
5. Mahalapye	0.261	4.705	0.000	0.428	3.698	0.007
6. Maun	0.348	4.071	0.003	0.613	6.677	0.000
7. Shakawe	0.447	4.678	0.001	−0.183	−1.748	0.093
8. Tsabong	0.209	4.961	0.000	0.365	5.016	0.000
9. Tshane	0.158	3.054	0.019	0.456	6.887	0.000

p values in bold show insignificant linear trends

climate variability in Southern Africa, Davis (2011) noted that annual T_{min} trend for the region was increasing at the rate of 0.27 °C per decade from 1976 to 2009. The disparity between the country average and that of the region is due to length of the time series considered. Trends calculated from short time series are often steeper than those from longer series (Tshiala et al. 2011). Besides, Davis (2011) note that 1970s were a period of rapid warming leading to steeper regional annual T_{min} trends. The country's annual T_{min} trends are, however, comparable to that observed in Egypt (partly semi-arid) which is 0.12 °C per decade over a 60-year period (Domroes and El-Tantawi 2005).

It can be also observed from Table 3 that warming rates in annual T_{min} at Ghanzi, Maun, Tsabong and Tshane (southern sand veldt stations) outpaced their respective annual T_{max} trends. Similarly, with the exception of Kasane, stations at the northern part of country exhibited significant warming rates in annual T_{max} which outstripped annual T_{min} magnitude. Kasane showed significant cooling in both annual T_{max} and T_{min}. Generally, about 67% of the stations showed steeper cooling or warming rates in annual T_{min} than respective annual T_{max}.

Thomas et al. (2000) and Reed et al. (2007) observed that the southern sand veldt region suffered significant rangeland degradation due to periodic droughts and poor land management practices (e.g., deforestation and livestock overgrazing) since 1950s. In a recent study, Dougill et al. (2016) observed that the moderate-resolution imaging spectroradiometer (MODIS) derived Normalized Difference Vegetation Index (NDVI) time series matched interannual rainfall variability in the region. This is corroborated by an observation that in southern African savannas, vegetation productivity is strongly influenced by precipitation (Chamaillé-Jammes and Fritz 2009). Furthermore, analysis of a more than 50-year (1950–2008)-long annual precipitation time series at the stations showed a general decreasing trend at the rate of −0.41 to −2.24 mm per annum (Batisani and Yarnal 2010; Mphale et al. 2014). This could suggest a decrease in vegetation productivity in the region as per the observation made by Dougill et al. (2016).

According to Zhou et al. (2007), a reduction in soil moisture content and vegetation productivity decreases land surface emissivity and increases land surface albedo, respectively. The changes in the land surface biophysical characteristics disturb local and regional climate as they alter land surface energy balance. Consequently, loss of vegetation cover/productivity and soil aridation in the region could have led to a significant reduction in land surface emissivity. Zhou et al. (2007) note that a decrease in land surface emissivity warms up T_{min} more than T_{max} which could explain the observed steeper increasing T_{min} trends than those of T_{max} in the arid and semi-arid region (Table 3). Correlation analysis between T_{max} and precipitations in the region shows a strong negative relationship ($r > 0.57$) between the parameters (Kenabatho et al. 2012).

There are concerns that woodland savannas of northern sand veldt region are undergoing large-scale land degradation due to intensifying fire frequency, deforestation, grazing and human population growth pressures (Heinl et al. 2006; Pricope et al. 2015). Land degradation map of Botswana shows that Francistown, Kasane and Shakawe have suffered severe-to-moderate degradation over the years (Reed et al. 2007). It is also noteworthy that Shakawe and Kasane are in Okavango and Chobe river Basins, respectively. The streamflows from the two rivers are strongly correlated with surface relative humidity (Table 4). The table also shows significant negative correlation between annual T_{max} and streamflow at Kasane. However, long-term trend analysis shows a decline in seasonal flood pulse discharges from both Chobe and Okavango rivers (Wolski et al. 2006; Gieske 1997). Nighttime radiative cooling due to large-scale deforestation and reduction of atmospheric water vapor has lead to decrease in annual T_{min} at the two stations.

Table 4 Annual streamflow trends for Kasane and Shakawe and correlation between streamflow with RH, T_{max} and T_{min}

Station	Streamflow trend (m^3 s^{-1}/10 years)	Correlation coefficient (r)		
		RH	T_{max}	T_{min}
1. Kasane	0.438[a]	0.581[a]	0.555[a]	−0.267
2. Shakawe	0.174	0.464[a]	−0.200	−0.012

[a] Signs indicate values at 95% confidence level

Mawalagedara and Oglesby (2012) note that deforestation results in two competing effects: cooling due to increase in surface albedo, and warming resulting from a decrease in evapotranspiration. Changes in land surface albedo at Kasane could have resulted in cooling during the day while the other effect was predominant at Francistown and Shakawe. This has lead to decreasing and increasing trends in annual T_{max} at the Kasane and Shakawe, respectively. Jonsson (2004) attributes cooling in annual T_{max} at Gaborone to small pockets/areas within the city with high vegetation densities leading to increases in evapotranspiration or oasis effect. Conversely, land surface degradation at Francistown could be attributable to the observed annual T_{max} trend. Urban heat island (UHI) and aerosols from pollution at the two developing cities could explain the detected warming in annual T_{min} (Jonsson et al. 2002).

4.4.2 *Seasonal T_{max} and T_{min} trends*

Table 5 shows a summary of seasonal T_{max} and T_{min} trends at the nine (9) stations. It can be inferred from the table that up to 78% of the stations had a significant positive trends in both the T_{max} and T_{min} during winter and spring (at 90% confidence level) The significant trends in T_{max} varied from 0.15 to 0.41 °C per decade while those in T_{min} ranged from 0.12 to 0.53 °C per decade. Majority of the stations in southern sand veldt had their steepest positive trends in T_{max} and T_{min} was during either winter or spring. The same is true for stations in the hard veldt. On the contrary, Kasane experienced significant cooling (at 90% confidence level) during all the seasons with steepest T_{max} and T_{min} trends occurring during autumn and winter, respectively. Shakawe also exhibited significant cooling in T_{min} during autumn and winter. The table also shows that the gentlest trends in T_{max} and T_{min} for most stations were during summer. Kasane and Gaborone had the gentlest trend in T_{min} during summer with their T_{max} trends were gentlest in spring and winter, respectively. The gentlest insignificant warming in T_{max} is at the rate of 0.03 °C per decade and was experienced at Ghanzi during summer. The steepest warming, determined to be at rate of 0.53 °C per decade, was in T_{min} during winter and was experienced at Maun.

Northern sand veldt stations experienced significant cooling in seasonal T_{min} during autumn and winter (Table 5). This could be due to reduction in cloud cover which consequently promoted radiative cooling at the surface (Jonsson et al. 2002). The decrease in cloud cover at Shakawe led to an increase in the amount of solar radiation at the surface during daytime, hence the observed increasing trend in T_{max}. Deforestation-induced increase in surface albedo decreased seasonal T_{max} at Kasane during all seasons (Mawalagedara and Oglesby 2012). For the aforementioned reason advanced for Shakawe, seasonal T_{min} also decreased through radiative cooling. Contrary to the observed T_{min} trends during autumn and winter, there was slight warming the variable during spring and summer. This could be attributed to increased cloud cover.

Table 5 Seasonal T_{max} and T_{min} trends

Station	T_{max}				T_{min}			
	Summer	Autumn	Winter	Spring	Summer	Autumn	Winter	Spring
1. Francistown	0.056	0.130[b]	0.176[b]	0.308[b]	0.064	0.043	0.117[a]	0.203[b]
2. Gaborone	−0.185[b]	−0.020	−0.013	0.077	0.005	0.014	0.192[b]	0.080
3. Ghanzi	0.034	0.073	0.170[b]	0.255[b]	0.089[a]	0.171[b]	0.206[b]	0.244[b]
4. Kasane	−0.429[b]	−0.544[b]	−0.360[b]	−0.253[a]	−0.277[b]	−0.790[b]	−0.959[b]	−0.932[b]
5. Mahalapye	−0.011	0.206[b]	0.165[b]	0.177[b]	0.058	0.314[b]	0.514[b]	0.456[b]
6. Maun	0.136	0.218[b]	0.409[b]	0.303[b]	0.478[b]	0.391[b]	0.528[b]	0.504[b]
7. Shakawe	0.156	0.258[b]	0.393[b]	0.323[b]	0.046	−0.275[b]	−0.264[b]	0.025
8. Tsabong	−0.126[a]	0.235[b]	0.201[b]	0.154[b]	0.288[b]	0.196[b]	0.176[b]	0.340[b]
9. Tshane	−0.129[a]	0.230[b]	0.281[b]	0.210[a]	0.212[b]	0.331[b]	0.434[b]	0.437[b]

[a, b] Signs indicate values at 90 and 95% confidence level, respectively

Significant warming (at 95% confidence level) in seasonal T_{min} was experienced at all southern sand veldt stations during the period of study. This could be attributable to decreases in land surface emissivity (e.g., in Zhou et al. 2007). However, significant warming in T_{min} (at 90% confidence level) was experienced predominantly during autumn, winter and spring for all the stations in the region. Significant cooling was experienced summer at Tshane and Tsabong during summer. This was due to availability of moisture for evapotranspiration during the season.

Significant warming was also experienced in seasonal T_{max} at most of the hard veldt stations during autumn, winter and spring. However, seasonal T_{min} was increasing mainly during winter and spring. Gaborone exhibited significant warning in T_{min} during winter and significant cooling during summer as observed in Jonsson (2004).

4.4.3 Annual and seasonal DTR trends

The results of the MK test on annual and seasonal DTR time series at the nine (9) stations are shown in Table 6. Contrary to the observed global DTR trend (Vose et al. 2005), the table shows significant warming trend in annual DTR at Francistown, Kasane, and Shakawe (at 90% confidence level). The warming trends varied from 0.25 to 0.67 °C per decade. The rest of the stations experienced cooling in the annual DTR at different levels of confidence. It can also be observed from the table that Gaborone, Mahalapye, Maun, Tsabong and Tshane experienced significant decreasing trends which ranged from −0.09 to −0.30 °C per decade at 95% confidence level. Insignificant decreasing trend was experienced at Ghanzi at the rate of −0.06 °C per decade. The observed opposite trends in DTR are corroborated by several studies, e.g., in New et al. (2006), Freiwan and Kadioğlu (2008), Tshiala et al. (2011) and Sayemuzzaman et al. (2015). When studying daily climate extreme over southern and West Africa, New et al. (2006) noted that annual DTR at some neighboring stations exhibited opposing trends. Zhou et al. (2009) ascribed the regional variance in DTR trends to changes in soil moisture and land cover biophysical properties (e.g., albedo and emissivity).

Table 6 Seasonal and annual *DTR* trends

Station	DTR				
	Summer	Autumn	Winter	Spring	Annual
1. Francistown	0.046	0.204[b]	0.145	0.173[b]	0.245[a]
2. Gaborone	−0.218[b]	−0.026	−0.174[b]	−0.008	−0.131[b]
3. Ghanzi	−0.007	−0.084	−0.169[a]	−0.015	−0.061
4. Kasane	−0.3043	0.452[b]	0.827[b]	0.706[b]	0.672[b]
5. Mahalapye	−0.014	0.022	−0.133[b]	−0.066	−0.297[b]
6. Maun	−0.102[a]	−0.109[a]	−0.304[b]	−0.151[b]	−0.296[b]
7. Shakawe	0.195[b]	0.355[b]	0.477[b]	0.427[b]	0.485[b]
8. Tsabong	−0.221[b]	−0.016	−0.032	−0.226[b]	−0.085[b]
9. Tshane	−0.239[b]	−0.040	−0.201[b]	−0.345[b]	−0.286[b]

[a, b] Signs show values at 90 and 95% confidence level, respectively

Table 6 shows that majority (about 90%) of the stations experienced a decline in DTR trends during summer. This was mainly due to either a decreasing trend in summer T_{max} or stronger warming in T_{min} than respective T_{max}. The stations which exhibited significant decrease in summer DTR trend are Gaborone, Kasane, Maun, Tsabong and Tshane. About 80% of rainfall in the country occurs during October to March and is mainly convective in nature (Scanlon et al. 2005). During this period, the region experiences low sunshine duration due to low rain-bearing convective clouds with high albedo which dampen T_{max} and amplify T_{min} (Dai et al. 1999). With regard to this, majority of the stations experienced reduction in summer T_{max}.

Moreover, Manatsa et al. (2015) observed significant negative correlation between change in DTR and change in cloud cover fraction in the region. Seasonal DTR trend decreased at the stations in the southern part of the country for all seasons ranging from −0.01 to −0.35 °C per decade. The highest significant cooling in seasonal DTR was in spring at Tshane while the gentlest was in summer at Ghanzi. The observation is corroborated by an observation in semi-arid Jordan in which Freiwan and Kadioğlu (2008) determined highest cooling of a similar magnitude during summer. Warming in seasonal DTR was observed at stations in the northern part of the country during all seasons except summer. The warming was significant in all seasons except at Francistown during winter and ranged from 0.05 to 0.83 °C per decade.

Most of the considered stations exhibit an increasing trend in the magnitude of DTR form summer to winter seasons. However, the increasing trend in DTR magnitude was from autumn to spring at Tsabong and Tshane. This could be alluded to the onset of wet season at the two stations, which comes later than other stations in the northern part of the country. It is noteworthy that the wet season in the country is mainly dependent on the seasonal migration of the Inter Tropical Convergence Zone (ITCZ) which reaches its southernmost position in March. Therefore, seasonal soil moisture content and atmospheric water vapor influence seasonal variation of DTR and T_{min} in the country. The maximum DTR trends at Shakawe and Kasane coincide with period when Okavango and Chobe rivers are at the peak of their flow discharges (Pricope et al. 2015).

4.5 T_{min}, T_{max} and DTR change points analysis

4.5.1 Lepage and SQMK tests

The results of the Lepage test for change points in annual T_{min} and T_{max} data at the nine (9) stations are shown in Fig. 3. The figure shows that during the period of study there were several change points in T_{min} and T_{max} time series, but the most significant coextensive change point for the variables at most of the stations was 1981. A few non-coincident change points occurred at Ghanzi, Shakawe and Tsabong. However, 1981 seemed to be a predominant change point for either annual T_{min} or T_{max}. Kenabatho et al. (2012) carried out a similar analysis with annual T_{min} and T_{max} at some of the stations using cumulative sums (CUSUM) technique and observed the change point to be 1981. Application of SQMK technique also confirmed the change point.

Kane (2009) note that El Niño episodes have been unusually recurrent since the late 1970s. This is attested by the significant changes in annual T_{max} trends in around 1976 at most of the considered stations (Fig. 3). However, this changed in the early 1980s when dry conditions were experienced throughout Southern Africa. A severe El Niño event occurred during 1982–1983 season which had catastrophic effect on vegetation through extremely high air temperatures and below-normal rainfall (Kane 2009). This created an extensive drought and severely water-stressed vegetation conditions throughout the subcontinent (Anyamba et al. 2002). This changed the trends in both annual T_{min} and T_{max} at the considered stations (see Fig. 3). The figure also shows that the most significant change point for when new opposite trends in both the annual T_{min} and T_{max} began is 1981. However, this was different for annual T_{min} at Kasane and Shakawe. The change point for the stations was observed to be 1991–1992. Kenabatho et al. (2012) also found the same change point for Shakawe.

SQMK method revealed that for most stations, the significant change point of annual DTR trends (DTR_{cp}) did not correspond with the coincident annual T_{min} and T_{max} change point (T_{cp}). It occurred a year or two after T_{cp} (Fig. 4). The most conspicuous DTR_{cp} for the considered stations is 1982–1983. This is not surprising as it coincided with the year of catastrophic El Niño event. Before the DTR_{cp}, DTR was increasing and conversely so after the change point for most of the stations (Figs. 5, 6). T_{max} was increasing at a faster rate compared to T_{min}. This could have been due to vegetation productivity changes and anomalous reduction of precipitation during this period (Wu et al. 2011). After the change point annual T_{min} trend was faster than T_{max} trend mainly because of the prevailing dry conditions over most of the regions.

Cloud cover is observed to influence both the T_{min} and T_{max} through back scattering of longwave radiation at night, thus increasing T_{min} and damping T_{max} by reflecting incoming shortwave radiation (Dai et al. 1997; Stone and Weaver 2003). Cloud cover fraction climatology for 1979–2010 and anomalies for before and after change points are shown in Fig. 7a–d. Figure 7a, b shows that before 1983, below-normal cloud cover prevailed over most parts of the country which predominantly increased T_{max} more than T_{min}. However, this changed soon after the year as the cloud cover increased over most stations with the reversal of the daily temperature regime, thus T_{min} outpacing T_{max}. For Shakawe and Kasane a similar situation developed just before and after 1993, year of their significant change point. Soon after 1993, northern Botswana experienced significant cloud cover with coincident increase in precipitation (Fig. 7c, 7d). This decreased T_{max} at both the stations.

The general wind field climatology for 1979–2010 is shown in Fig. 8a. The position of the St. Helena and South Indian High pressure cells influenced wind patterns and moisture fluxes into the subcontinent during this period. It could be seen from the figure that there was generally a low-pressure system aligned along the northwest–southeast axis. An anticyclonic circulation which is normally centered in southern Mozambique channel moved inland westward with further intrusion of moist air during the period. Before 1983, a strong high-pressure circulation developed over southern Angola which promoted the influx of cold dry air flow through Namib and Kalahari deserts to most parts of the country (Fig. 8b). Consequently, dry conditions prevailed over the country which desiccated vegetation and decreased land surface emissivity. However, soon after the change point, atmospheric circulation reversed as an intense low-pressure system developed over southern Angola and northern Namibia. This facilitated the intrusion of warm moist air from south eastern Atlantic Ocean, a condition associated with wet condition over the subcontinent (Reason and Smart 2015). In a period before 1993 (1979–1992), an intense high system developed over southern Angola with effects as discussed above. After 1993, an anomalous low-pressure system developed over Southern Africa affecting most parts of the country (Fig. 8e). This brought about above-average precipitation over most of the stations except Tshane and Tsabong.

The influence of vegetation greenness on T_{max} stands out during the periods before the change points. Increase in precipitation in arid and semi-arid regions can be associated with increase in vegetation productivity, e.g., in Zhang et al. (2016). Since precipitation was low before change points, negative feedback of vegetation decrease increased T_{max} at all stations. T_{max} was more influenced by vegetation decrease than T_{min} at most stations (Wu et al. 2011).

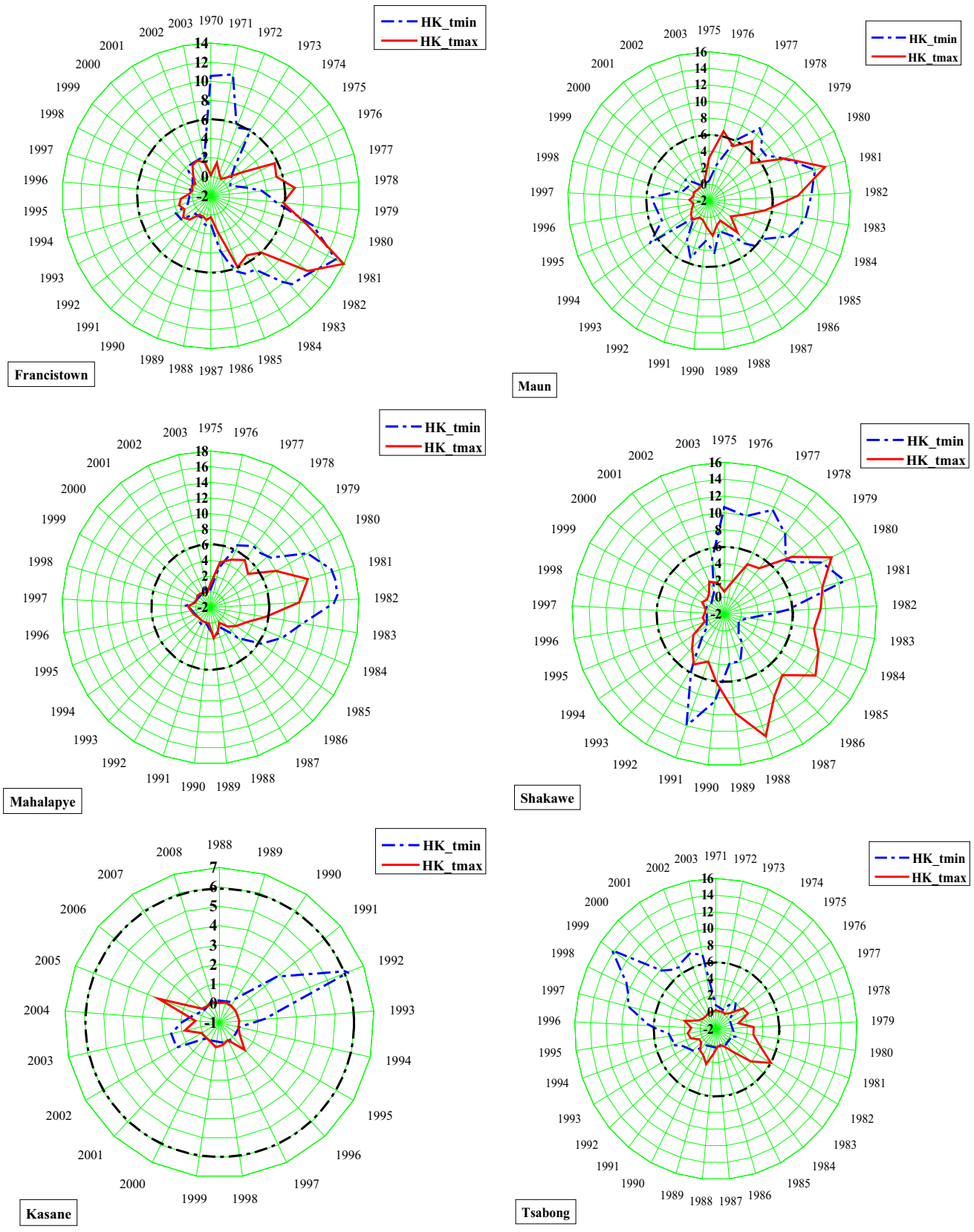

Fig. 3 Annual T_{max} and T_{min} change points determined using Lepage test for stations: Francistown, Kasane, Mahalapye, Maun, Tsabong and Tshane

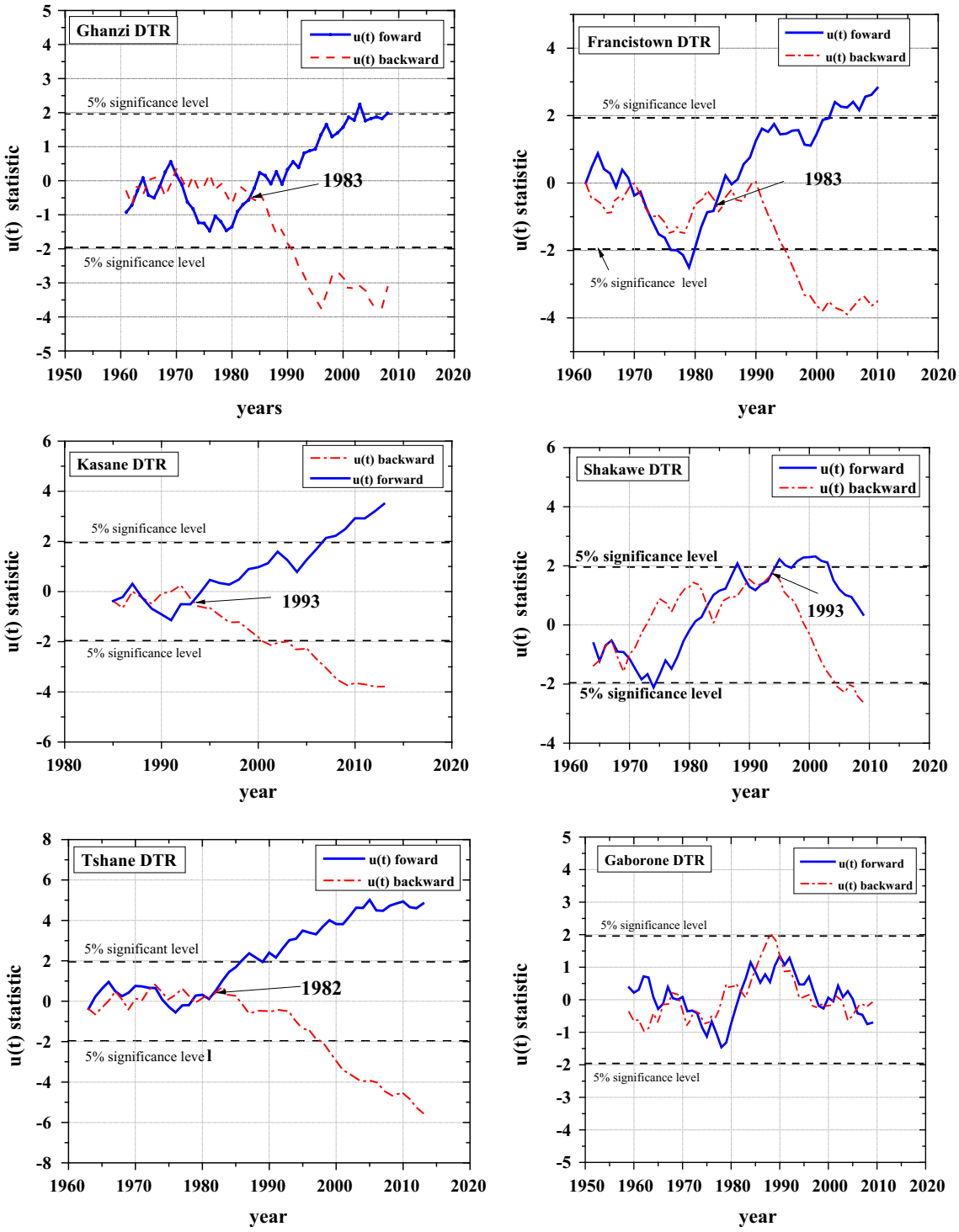

Fig. 4 DTR change points for Francistown, Gaborone, Ghanzi, Kasane, Tsabong, Tshane and Shakawe

Continued loss of vegetation productivity and soil aridation increased the trend of T_{min} just after the change point, i.e., change of temperature regime from T_{max}-trend-dominated to T_{min}-trend-dominated. However, increase in precipitation decreased T_{max} trend through damping effect of clouds and evapotranspiration after the change points. Increased cloud cover amplified the nighttime temperature (T_{min}).

In Kasane, increase in vegetation greenness due to increase in precipitation after the change point increased the evapotranspiration and land surface emissivity (Fig. 6).

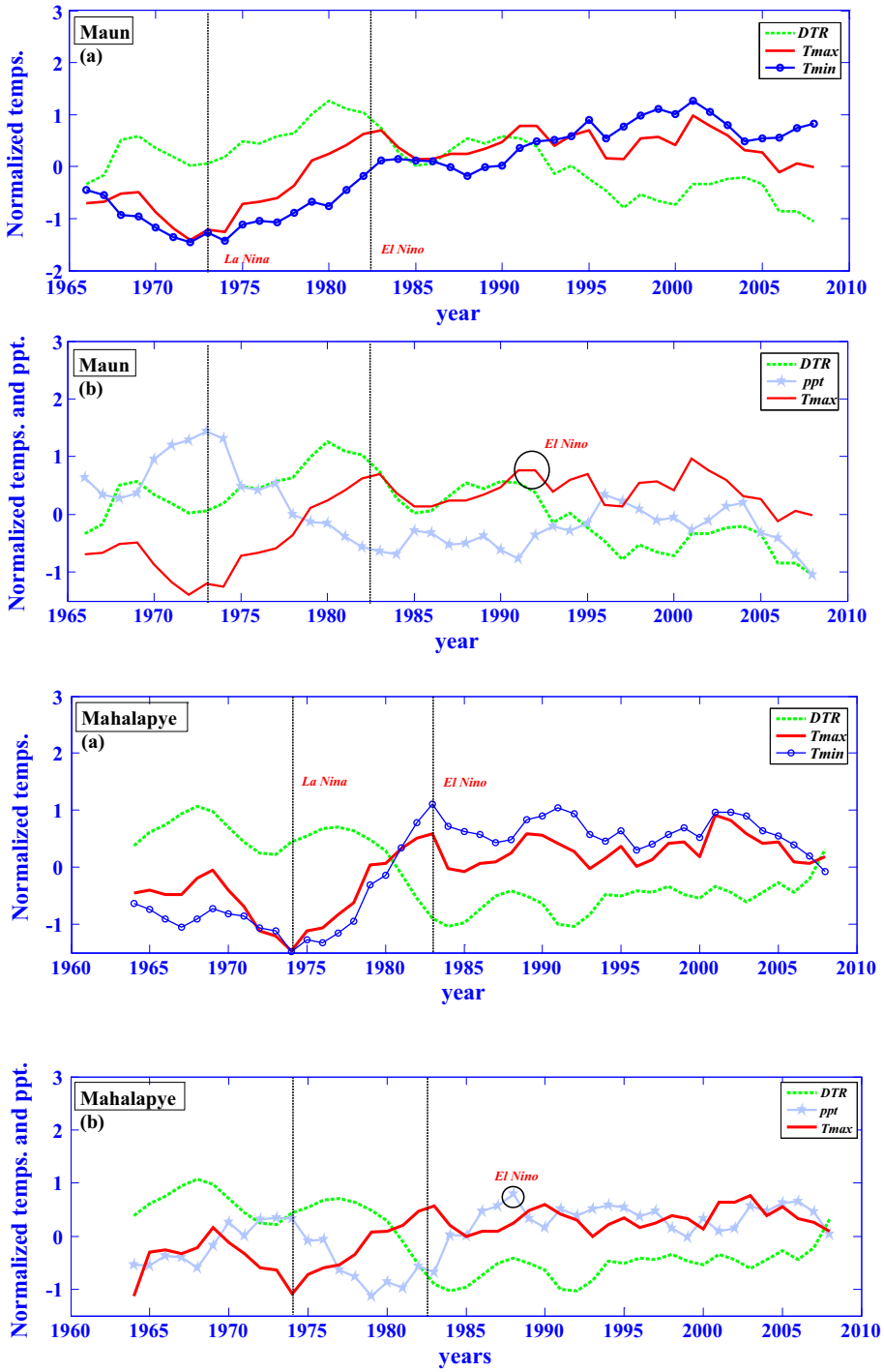

Fig. 5 Annual variation of T_{max}, T_{min}, DTR and precipitation for Mahalapye and Maun (*black dashed lines* denote positions for temperature trend change points)

The combined effect of evapotranspiration-induced cooling and cloud damping of incident solar radiation reduced daytime temperatures. However, deforestation permitted radiative heat loss from the land surface. Annual T_{max} outpaced annual T_{min}, hence the observed negative trend in DTR during this period. Before the change point, there was an increasing trend in T_{max} due to decrease in cloud cover and influx of cold dry air from the Namib desert which inhibited precipitation over the country. Low vegetation productivity and soil moisture deficiency during this period promoted radiative heat energy loss from the ground surface rate, hence the observed negative trends in T_{min}. This lead to increase in DTR during this period. Rainfall deficiency and deforestation over Shakawe resulted in increases in both the annual T_{min} and T_{max} before 1992. The rate of increase in of T_{max} outpaced T_{min} leading a positive in DTR. The coincident increase in both cloud cover and rainfall after the change point decreased T_{max} and amplified

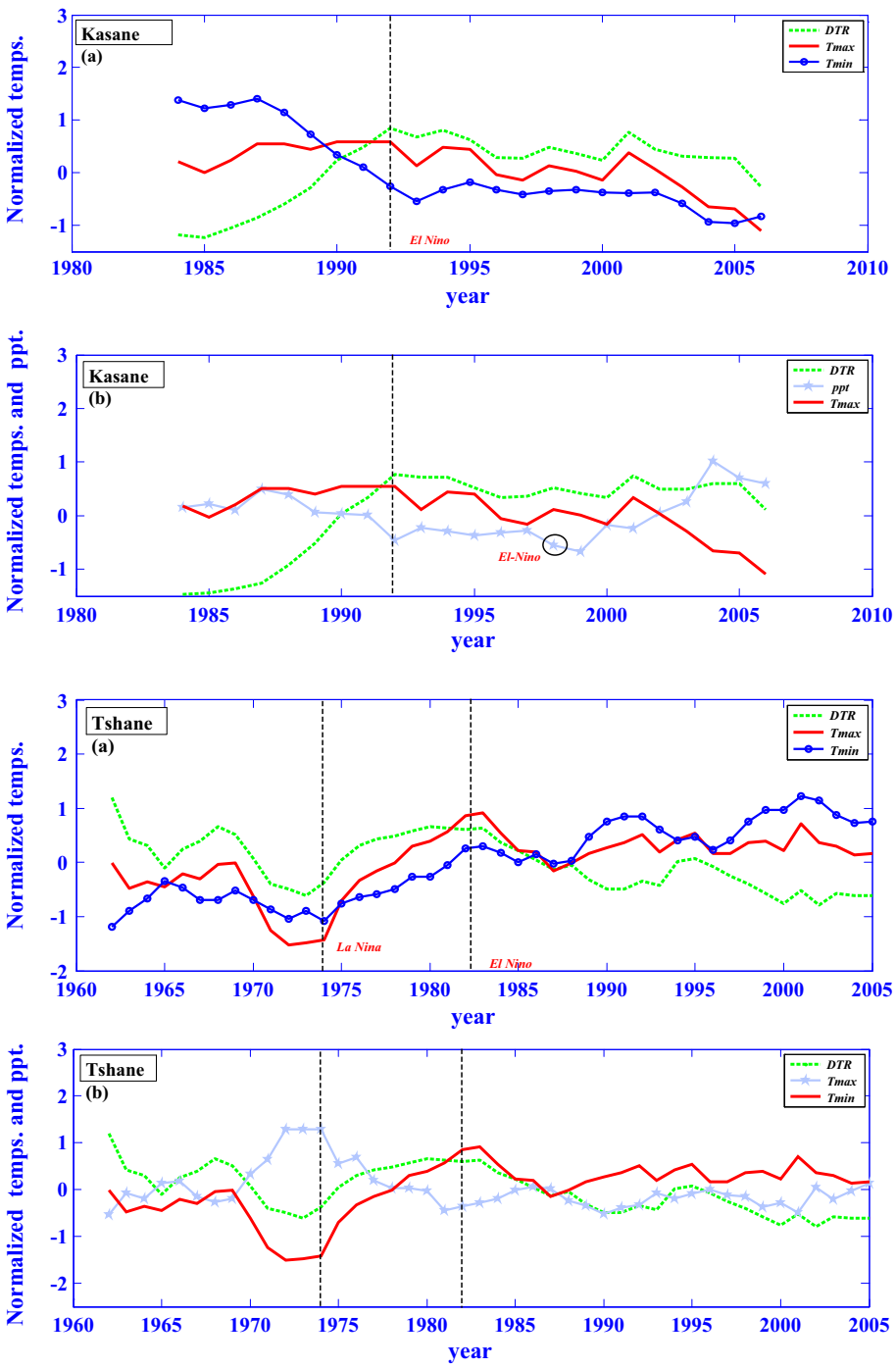

Fig. 6 Annual variation of normalized T_{max}, T_{min}, DTR and precipitation for Kasane and Tshane (*black dashed lines* denote positions for temperature trend change points)

T_{min}. Rate of increase in T_{min} outpaced the negative trend in T_{max} leading to increasing trend in DTR at the station.

Precipitation deficit and low cloud cover could explain observed trends in both annual T_{min} and T_{max} at Francistown and Mahalapye before 1982. As annual T_{min} outpaced T_{max}, a downward trend in DTR was observed. After the change point, cloud cover, radiative heat loss and evapotranspiration-induced cooling lowered both T_{max} and T_{min}.

5 Conclusions

A normality test on homogeneous annual T_{max} and T_{min} time series from the selected stations has shown that the series conformed to Gaussian distribution at 95% confidence level as the absolute values of the coefficients of skewness and kurtosis were less than 1.96. This implied that the parametric simple regression and non-parametric

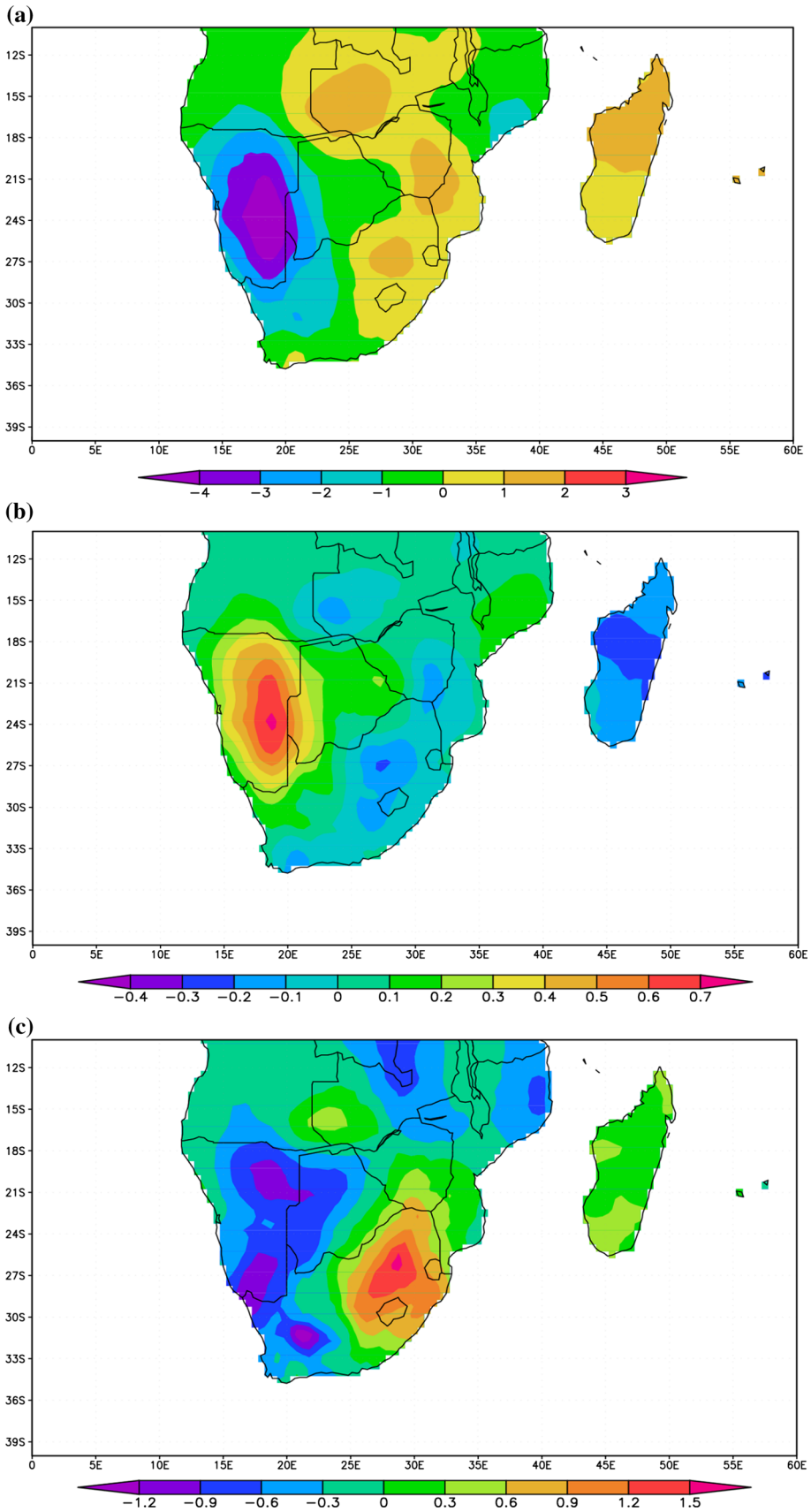

Fig. 7 CRU cloud cover for: **a** (1979–1983) minus (1979–2010) anomaly; **b** (1984–2010) minus (1979–2010) anomaly; **c** (1979–1992) minus (1979–2010) anomaly and (1993–2010) minus (1979–2010) anomaly

Fig. 7 continued

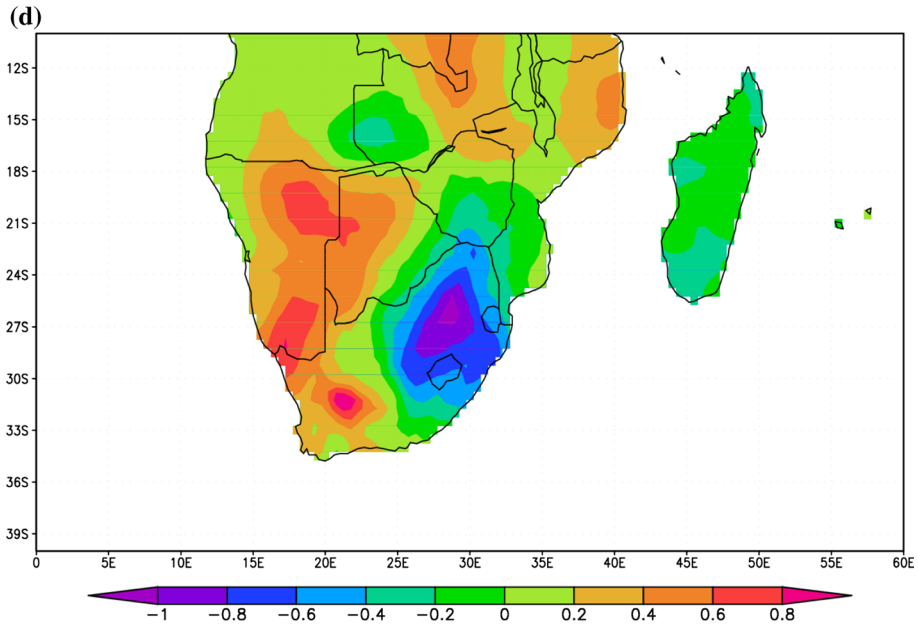

MK methods were both suitable for trend analysis of temperature.

The application of both trend tests on the homogenized time series revealed that about 78% of the stations experienced significant (p value <0.1) positive trends in annual T_{max} at the rate of 0.14–0.45 °C per decade. The rate of increase of the T_{max} is within the calculated regional trend as determined by Davis (2011). In semi-arid areas, vegetation productivity is strongly influenced by precipitation (Fensholt et al. 2012). Consequently, a decrease in precipitation may imply a decrease in soil moisture as well as vegetation productivity in the semi-arid areas, e.g., in Miranda et al. (2011). A decrease in vegetation productivity leads to a decrease in evapotranspiration. Besides, Wang et al. (2014) note that soil moisture and evapotranspiration have a cooling effect on T_{max}. Thus, the observed significant positive trends in annual T_{max} could be ascribed to negative trends in precipitation and evapotranspiration at most the stations over the last few decades (Batisani and Yarnal 2010). Significant cooling in annual T_{max} at the rate of −0.52 °C per decade was experienced in Kasane. According to a land degradation map of Botswana, Kasane is experiencing a severe land degradation and deforestation (Reed et al. 2007). These effects on vegetation are attributable to increasing human and wildlife population pressure and high wildfire incidences in the region (Pricope et al. 2015). According to Nduwayezu et al. (2015), human encroachment and elephants are responsible for an average of about 60% tree mortality rate in the region. The land degradation and deforestation have resulted in land surface albedo increase and consequently a decrease in its net solar radiation hence the observed cooling effect on T_{max}. The cooling effect offsets the warming due decrease in evapotranspiration (see Li et al. 2013).

About 56% of the stations experienced significant (p value <0.01) warming in annual T_{min} at the rate of positive trend ranged from 0.25 to 0.61 °C per decade. These stations are in semi-arid shrub savanna ecosystems where soil moisture and precipitation are the major factors that control land surface temperature. In most cases, clouds that develop over the region of study are rain-bearing (Manatsa et al. 2015). Thus, reduction in precipitation over the study period implies a decrease in cloud cover fraction. Consequently, there was an increase of net surface radiation stored at the land surface which was released at sensible heat at night which results in the observed positive trend in T_{min}. On the other hand, a significant ($p < 0.01$) cooling in annual T_{min} at the rates of −0.18 and −0.87 °C per decade were experienced at Shakawe and Kasane, respectively. It is observed that the two stations are in dry deciduous forests and undergoing moderate-to-severe deforestation as aforementioned. The removal of vegetation causes intense land surface heating during the day and intense terrestrial radiation loss from the moisture-deficient low thermal inertia soils at night (e.g., in Yadav et al. 2004).

The tests also revealed that about 78% of the stations exhibited significant (at 5% significance level) positive trends in both the seasonal T_{max} and T_{min} during dry seasons. The significant trends in seasonal T_{max} ranged from 0.15 to 0.41 °C per decade while that of seasonal T_{min} varied from 0.12 to 0.53 °C per decade. As mentioned above soil moisture is the main biophysical factor that controls land surface temperature. During austral summer,

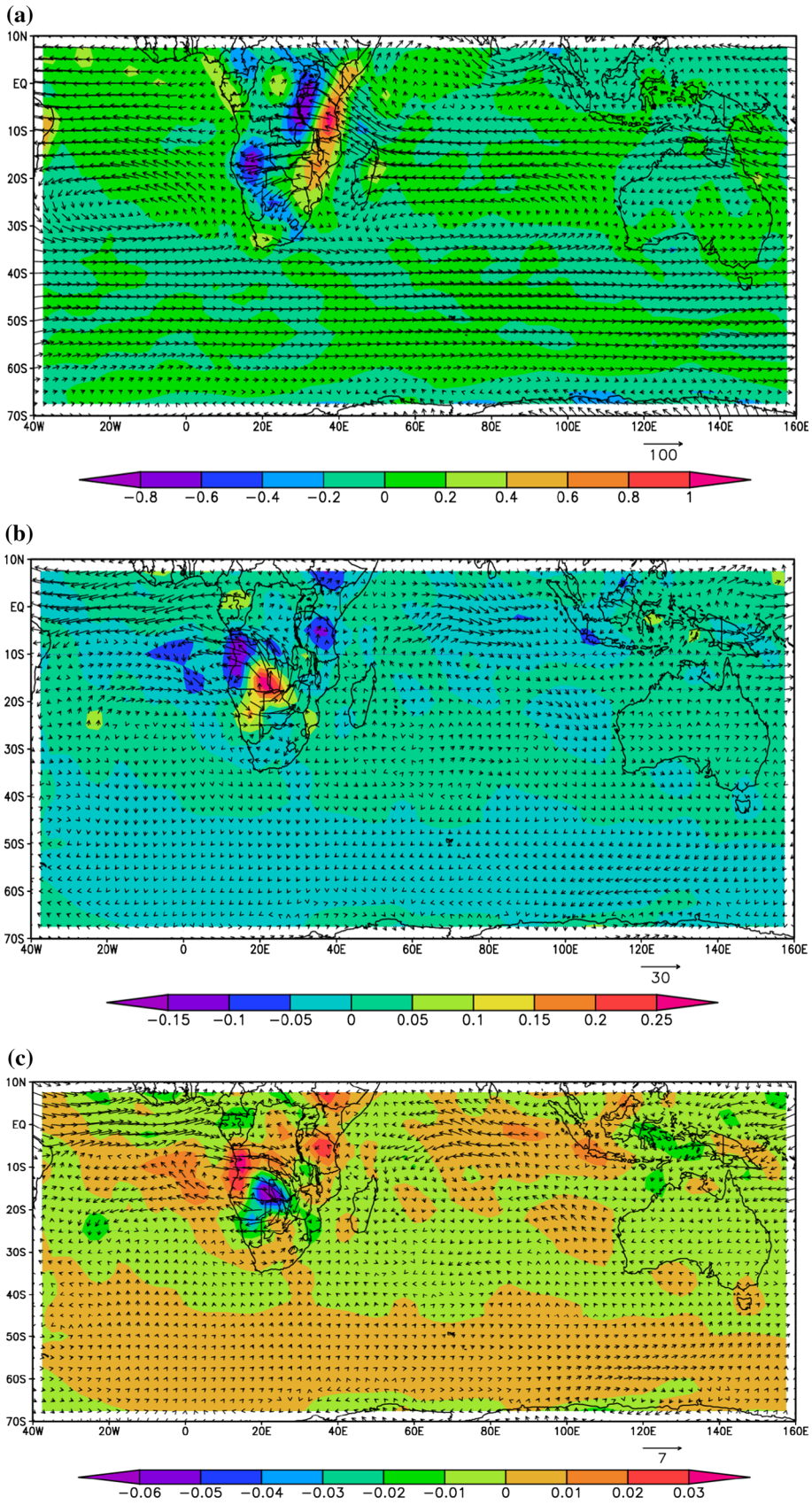

Fig. 8 NCEP wind patterns and divergence for: **a** 1979–2010; **b** (1979–2010) minus (1979–1983) anomaly; **c** (1979–2010) minus (1984–2010) anomaly; **d** (1979–2010) minus (1979–1991) anomaly and **e** (1979–2010) minus (1992–2010)

Fig. 8 continued

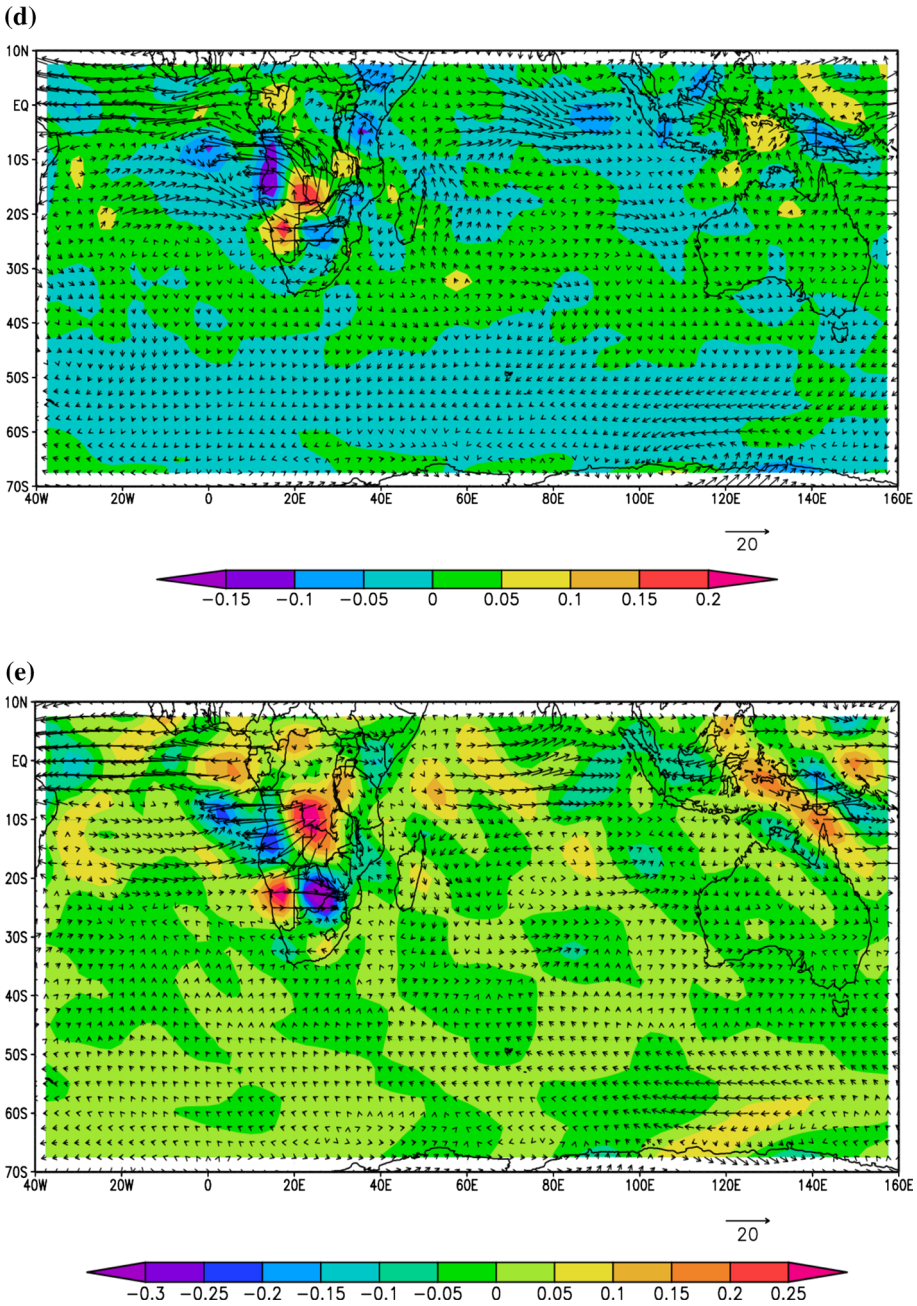

most stations receive ITCZ-influenced precipitation which increases soil moisture. Over the years, the amount of soil moisture due to rainfall decreased. Thus, the positive trends in both summer T_{max} and T_{min} compared other seasons.

The warming rates in annual T_{min} at stations in the southern part of the country (Ghanzi, Mahalapye, Maun, Tsabong and Tshane) outpaced their respective annual T_{max} trends, resulting in significant negative trends in annual DTR. The warming in the annual DTR ranged from −0.09 to −0.30 °C per decade (at 95% confidence level). There has been aridation in the station due to decreased precipitation. Soil degradation and erosion by wind increased aerosol loading in the atmosphere. The backscattering of longwave radiation from the ground surface amplified the T_{min}.

Stations in the northern part of the country experienced positive trends in annual DTR brought about by either a decreasing annual T_{min} trend which outstrips annual T_{max} or annual T_{max} outpacing annual T_{min}. The warming trends varied from 0.25 to 0.67 °C per decade (at 90% confidence level). Deforestation has two competing effects during daytime: warming due to decrease in evapotranspiration and the cooling effect due to increase in land surface albedo. In the case of Shakawe, the warming effect offset the effect due to increase in the land surface albedo.

Majority (about 90%) of the considered stations experienced a decreasing DTR trends during summer. This was mainly due to either a decreasing trend in summer T_{max} or stronger warming in T_{min} than its respective T_{max}. Soil moisture influences DTR trend at almost all stations in the country through T_{max}. Seasonal DTR trend decreased at the stations in the southern part of the country for all seasons ranging from −0.01 to −0.35 °C per decade.

Analysis of change points in T_{max}, T_{min} and DTR time series using Lepage test and SQMK has revealed that there exist several change points in T_{min} and T_{max} time series, but the most significant coextensive change point at most of the stations was 1981. There were frequent El Niños which affected the Southern Africa since the late 1970s (Kane 2009). However, prevalent dry conditions which significantly affected soil moisture at most of the stations were in the year 1981. The conditions had a significant influence on both T_{min} and T_{max} (Kenabatho et al. 2012).

For most of the stations, the most significant change point of annual DTR trends did not correspond with the coincident annual T_{min} and T_{max} change points. It occurred a year or two after, 1982/1983 as the most conspicuous. The most intense El Niño was in 1982/1983 season, when the difference in T_{min} and T_{max} (DTR) was most significant.

Precipitation deficit and changes in vegetation productivity could be a possible explanation of change in the trends of T_{max}, T_{min} and DTR time series. Before 1983, a strong anticyclonic circulation developed over southern Angola which promoted the influx of cold dry air flow over Namib and Kalahari deserts to most parts of Botswana. This consequently led to dry conditions over the country which desiccated vegetation and decreased land surface emissivity. After the change point, atmospheric circulation reversed as an intense low-pressure system developed over southern Angola and northern Namibia. This facilitated the intrusion of warm moist air from south eastern Atlantic Ocean, a condition associated with wet condition over the subcontinent.

References

Anyamba A, Tucker CJ, Mahoney R (2002) El Nino to La Nina: vegetation response patterns over East and Southern Africa during 1997–2000 period. J Clim 15:3096–3103

Batisani N, Yarnal B (2010) Rainfall variability and trends in semi-arid Botswana: implications for climate change adaptation policy. Appl Geogr 30:483–489

Bisai D, Chatterjee S, Khan A, Barman NK (2014) Application of sequential Mann–Kendall test for detection of approximate significant change point in surface air temperature for Kolkata weather observatory, West Bengal, India. Int J Curr Res 6:5319–5324

Blain GC (2013) The Mann–Kendall test the need to consider the interaction between serial correlation and trend. Acta Sci Agron 36:393–402

Boretti A (2013) A statistical analysis of the temperature records for the Northern Territory of Australia. Theor Appl Clim 114:567–573

Borges PA, Franke J, do Santos Silva FD, Weiss H, Bernhofer C (2014) Differences between two climatological periods (2001–2010 vs. 1971–2000) and trend analysis of temperature and precipitation in Central Brazil. Theor Appl Climatol 116:191–202

Brazel SW, Balling RC (1986) Temporal analysis of atmospheric moisture level in Phoenix, Arizona. J Clim Appl Meteorol 25:112–117

Brunetti M, Buffoni L, Maugeri M, Nanni T (2000) Trends of minimum and maximum daily temperatures in Italy from 1865 to 1996. Theor Appl Climatol 66:49–60

Buishand TA (1982) Some methods for testing the homogeneity of rainfall records. J Hydrol 58:11–27

Chamaillé-Jammes S, Fritz H (2009) Precipitation–NDVI relationships in eastern and southern African savannas vary along a precipitation gradient, Int J Remote Sens 30:3409–3422

Chatterjee S, Dipak Bisai D, Ansar Khan A (2014) Detection of approximate potential trend turning points in temperature time series (1941–2010) for Asansol Weather Observation Station, West Bengal, India. Atmos Clim Sci 4:64–69

Chernoff H, Zacks S (1964) Estimating the current mean of a normal distribution which is subject to changes in time. Ann Math Stat 35:999–1018

Chipanshi AC, Chanda R, Totolo O (2003) Vulnerability assessment of the maize and sorghum crops to climate change in Botswana. Clim Chang 61:339–360

Dai A, DelGenio AD, Fung IY (1997) Clouds, precipitation and temperature range. Nature 386:665–666

Dai A, Trenberth KE, Karl TR (1999) Effects of clouds, soil moisture, precipitation, and water vapor on diurnal temperature range. J Clim 12:2451–2473

Darkoh MBK (1999) Desertification in Botswana. In: Arnalds O, Archer S (eds) Case studies of Rangeland. Agricultural Research Institute, Reykjavik, pp 61–74

Davis C (ed) (2011) Climate risk and vulnerability: a handbook for southern Africa. CSIR, Pretoria. http://www.rvatlas.org/SADC. Accessed 20 July 2016

del Rio S, Fraile R, Herrero L, Penas A (2007) Analysis of recent trends in mean maximum and minimum temperatures in a region of the NW of Spain (Castilla y Leon). Theor Appl Climatol 90:1–12

Domroes M, El-Tantawi A (2005) Recent temporal and spatial temperature changes in Egypt. Int J Climatol 25:51–63

Dougill AJ, Akanyang L, Perkins JS, Eckardt FD, Stringer LC, Favretto N, Atlhopheng J, Mulale K (2016) Land use, rangeland degradation and ecological changes in the southern Kalahari, Botswana. Afr J Ecol 54:59–67

Douglas EB, Vogel RM, Knoll CN (2000) Trends in floods and low flows in the United States: impact of serial correlation. J Hydrol 240:90–105

Easterling DR, Horton B, Jones PD, Peterson TC, Karl TR, Parker DE, Salinger MJ, Razuvayev V, Plummer N, Jamason P (1997) Maximum and minimum temperature trends for the globe. Science 277:364–367

Fensholt R, Langanke T, Rasmussen K, Reenberg A, Prince SD, Tucker C, Scholes RJ, Le QB, Bondeau A, Eastman R, Epstein H, Gaughan AE, Hellden U, Mbow C, Olsson L, Paruelo J, Schweitzer C, Seaquist J, Wessels K (2012) Greenness in semi-arid areas across the globe 1981–2007—an earth observing

satellite based analysis of trends and drivers. Remote Sens Environ 121:144–158
Freiwan M, Kadioğlu M (2008) Climate variability in Jordan. Int J Climatol 28:69–89
Gajić-Čapka M, Zaninović K (1997) Changes in temperature extremes and their possible causes at the SE boundary of the Alps. Theor Appl Climatol 57(1–2):89–94
Gieske A (1997) Modeling outflow from the Jao/Boro river system in the Okavango Delta, Botswana. J Hydrol 193:214–239
Heinl M, Neuenschwander A, Sliva J, Vanderpost C (2006) Interactions between fire and flooding in a southern African floodplain system (Okavango Delta, Botswana). Landsc Ecol 21:699–709
Inthichack P, Nishimura Y, Fukumoto Y (2013) Diurnal temperature alterations on plant growth and mineral absorption in eggplant, sweet pepper and tomato. Hortic Environ Biotechnol 54:37–43
IPCC (2013) Summary for policymakers. In: Stocker TF, Qin D, Plattner GK, Tignor M, Allen SK, Boschung J, Nauels A, Xia Y, Bex V, Midgley PME (eds) Climate change 2013: the physical science basis. Contribution of working group i to the fifth assessment report of the intergovernmental panel on climate change. Cambridge University Press, Cambridge, pp 37–38
Jonsson P (2004) Vegetation as an urban climate control in the subtropical city of Gaborone, Botswana. Int J Climatol 24:1307–1322
Jonsson PH, Eliasson I, Lindqvist S (2002) Urban climate and air quality in tropical cities. In: Urban air pollution (joint with the fourth symposium urban environment), 12th joint conference on application of air pollution meteorology, Norfolk, VA
Kadioğlu M, Şaylan L (2001) Trends of growing degree-days in Turkey. Water Air Soil Pollut 126:83–96
Kalnay E, Kanamitsu M, Kistler R, Collins W, Deaven D, Gandin L, Iredell M, Saha S, Woollen J, Zhu Y, Chelliah M, Ebiszaki W, Higgins W, Janowiak J, Mo KC, Ropelewski C, Wang J, Leetmaa A, Reynolds R, Jenne R, Joseph D (1996) The NCEP–NCAR 40 year reanalysis project. Bull Am Meteorol Soc 77:437–471
Kane R (2009) Periodicities, ENSO effects and trends of some South African rainfall series—an update. S Afr J Sci 105(5–6):199–207
Kenabatho PK, Parida BP, Moalafhi DB (2012) The value of larger scale climate variables in climate change assessment: the case of Botswana's rainfall. Phys Chem Earth 50:64–71
King'uyu SM, Ogallo LA, Anyamba EK (2000) Recent trends of minimum and maximum surface temperatures over eastern Africa. J Clim 13:2876–2886
Knežević S, Tošić I, Pejanović G (2014) The influence of the East Atlantic oscillation to climate indices based on daily minimum temperatures in Serbia. Theor Appl Climatol 116:435–446
Kruger AC, Shongwe S (2004) Temperature trends in South Africa: 1960–2003. S Afr Int J Climatol 24:1929–1945
Legwaila GM, Mojeremane W, Madisa ME, Mmolotsi RM, Rampart M (2011) Potential of traditional food plants in rural household food security in Botswana. J Hortic For 3(6):171–177
Li Z, Deng X, Shi Q, Ke X, Liu Y (2013) Modeling the impacts of boreal deforestation on the near-surface temperature in European Russia. Adv Meteorol 486962:1–9
Liu X, Yin Z-Y, Shao X, Qin N (2006) Temporal trends and variability of daily maximum and minimum, extreme temperature events, and growing season length over the eastern and central Tibetan Plateau during 1961–2003. J Geophys Res 111:D19109. doi:10.1029/2005JD006915
Liu Y, Huang G, Huang RH (2011) Inter-decadal variability of summer rainfall in Eastern China detected by the Lepage test. Theor Appl Climatol 106:481–489
Madzwamuse M, Schuster B, Nherera B (2007) The real jewels of the Kalahari. Drylands ecosystem goods and services in Kgalagadi South District, Botswana. IUCN the World Conservation Union, France. http://www.cbd.int/financial/values/botswana-valueservices.pdf. Accessed 6 Jun 2014
Malema BW (2012) Botswana's formal economic structure as a possible source of poverty: are there any policies out of this economic impasse? PULA Botsw J Afr Stud 26:51–69
Manatsa D, Morioka Y, Behera SK, Mushore TD, Mugandani R (2015) Linking the Southern annular mode to diurnal temperature range over southern Africa. Intern J Climatol 35:4220–4236
Mavhura E, Manatsa D, Mushore T (2015) Adaptation to drought in arid and semi-arid environments: case of the Zambezi Valley, Zimbabwe. Jàmbá J Disaster Risk Stud 7(1):1–7
Mawalagedara R, Oglesby RJ (2012) The climatic effects of deforestation in South and Southeast Asia. In: Moudinho P (ed) Deforestation around the World. Intech, China
McMichael T, Montgomery H, Costello A (2012) Health risks, present and future, from global climate change. BMJ 344:e1359
Meehl GA, Stocker TF, Collins WD, Friedlingstein P, Gaye AT, Gregory JM, Kitoh A, Knutti R, Murphy JM, Noda A, Raper SCB, Watterson IG, Weaver AJ, Zhao ZC (2007) Global climate projections. In: Solomon S, Qin D, Manning M, Chen Z, Marquis M, Averyt KB, Tignor M, Miller HL (eds) Climate change 2007: the physical science basis: Contribution of working group I to the fourth assessment report of the intergovernmental panel on climate change. Cambridge University Press, Cambridge, pp 747–845
Miranda JD, Armas C, Padilla FM, Pugnaire FI (2011) Climatic change and rainfall patterns: effects on semi-arid plant communities of the Iberian Southeast. J Arid Environ 75:1302–1309
Modarres R, Sarhadi A (2009). Rainfall trends analysis of Iran in the last half of the twentieth century. J Geophys Res 114. doi:10.1029/2008JD010707(D03101)
Modarres R, Silva VPR (2007) Rainfall trends in arid and semi-arid regions of Iran. J Arid Environ 70:3190–3333
Mogotsi K, Moroka AB, Sitang O, Chibua R (2011) Seasonal precipitation forecasts: agro-ecological knowledge among rural Kalahari communities. Afr J Agric Res 6:916–922
Moraes JM, Pellegrino GQ, Ballester MV, Martinelli LA, Victoria RL, Krusch AV (1998) Trends in hydrological parameters of a southern Brazilian watershed and is relation to human induced changes. Water Resour Manag 12:295–311
Moreki JC, Tsopito CM (2013) Effect of climate change on dairy production in Botswana and its suitable mitigation strategies. Online J Anim Feed Res 3(6):216–221
Mphale KM, Dash SK, Adedoyin A, Panda SK (2014) Rainfall regime changes and trends in Botswana Kalahari Transect's late summer precipitation. Theor Appl Climatol 116:75–91
Naidoo S, Davis C, Archer van Garderen E (2013) Forests, rangelands and climate change in southern Africa. In: Forests and climate change working paper no. 12. Food and Agriculture Organization of the United Nations, Rome
Nasri M, Modarres R (2009) Dry spell trend analysis of Isfahan province, Iran. Int J Climatol 29:1430–1438
Nduwayezu JB, Mafoko GJ, Mojeremane W, Mhaladi LO (2015) Vanishing multipurpose indigenous trees in Chobe and Kasane forest reserves of Botswana. Resour Environ 5:167–172
New M et al (2006) Evidence of trends in daily climate extremes over southern and West Africa. J Geophys Res 111:D14102. doi:10.1029/2005JD006289
Nfila RB, Jain P (2011) Managing indigenous knowledge systems in Botswana using information and communication technologies. In: A paper presented at the 1st annual conference at the Faculty of Communication and Information Science and Technology, National University of Science and Technology (NUST), Bulawayo, 23–24 Aug 2011
Partal T, Kahya E (2006) Trend analysis in turkish precipitation data. J Hydrol Process 20:2011–2026

Pricope NG, Gaughan AE, All JD, Binford MW, Rutina LP (2015) Spatio-temporal analysis of vegetation dynamics in relation to shifting inundation and fire regimes: disentangling environmental variability from land management decisions in a southern African transboundary watershed. Land 4:627–655

Reason CJC, Smart S (2015) Tropical south east Atlantic warm anomalies over southern Africa. Front Environ Sci 3:1–11

Reed MS, Dougill AJ, Taylor MJ (2007) Integrating local and scientific knowledge for adaptation to land degradation: Kalahari rangeland management options. Land Degrad Dev 18:249–268

Reed MS, Stringer LC, Dougill AJ, Perkins JS, Atlhopheng JR, Mulale K, Favretto N (2015) Reorienting land degradation towards sustainable land management: linking sustainable livelihoods with ecosystem services in rangeland systems. J Environ Manag 151:472–485

Rockström J (2000) Water resources management in smallholder farms in eastern and Southern Africa: an overview. Phys Chem Earth 25:275–283

Rodionov S (2005) A brief overview of the regime shift detection methods. In: Large-scale disturbances (regime shifts) and recovery in aquatic systems, UNESCO ROSTE/BAS workshop on regime shifts, Varna, 14–16 June 2005, pp 17–24

Rodrigo FS, Esteban-Parra MJ, Pozo-Vázquez D, Castro-Diez Y (1999) A 500-year precipitation record in southern Spain. Int J Climatol 19:1233–1253

Saboohi R, Soltani S, Khodagholi M (2012) Trend analysis of temperature parameters in Iran. Theor Appl Climatol 109:529–547

Safari B (2012) Trend analysis of mean annual temperature in Rwanda during last fifty two years. J Environ Protect 3:538–551

Sayemuzzaman M, Mekonnen A, Jha M (2015) Diurnal temperature range trend over North Carolina and the associated mechanisms. Atmos Res 160:99–108

Scanlon TM, Caylor KK, Manfreda S, Levin SA, Rodriguez-Iturbe I (2005) Dynamic responses of grass cover to rainfall variability implication for function and persistence of savanna ecosystems. Adv Water Resour 28:291–302

Shahid S, Hazarika MK (2010) Groundwater droughts in the northwestern districts of Bangladesh. Water Resour Manag 24(10):1989–2006

Shahid S, Harun S, Katimon A (2012) Changes in diurnal temperature range in Bangladesh during the time period 1961–2008. Atmos Res 118:260–270

Stone D, Weaver A (2003) Factors contributing to diurnal temperature range trends in twentieth and twenty-first century simulations of the CCCma coupled model. Clim Dyn 20:435–445

Stringer LC, Dyer J, Reed M, Dougill A, Twyman C, Mkwambisi D (2009) Adaptations to climate change, drought and desertification: insights to enhance policy in southern Africa. Environ Sci Policy 12:748–765

Tabari H, Talaee PH (2011) Analysis of trends in temperature data in arid and semi-arid regions of Iran. Global Planet Change 79:1–10

Tabari H, Somee BS, Zadeh MR (2011) Testing for long-term trends in climatic variables in Iran. Atmos Res 100:132–140

Tabari H, Hosseinzadeh Talaee P, Ezani A, Shifteh Some'e B (2012) Shift changes and monotonic trends in autocorrelated temperature series over Iran. Theor Appl Climatol 109:95–108

Tadross M, Jack C, Hewitson B (2005) On RCM-based projections of change in southern African summer climate. Geophys Res Lett 32:L23713

Thomas DSG, Sporton D, Perkins JS (2000) The environmental impact of livestock ranches in the Kalahari, Botswana: natural resource use, ecological change and human response in a dynamic dryland system. Land Degrad Dev 11:327–341

Toreti A, Desiato F (2007) Temperature trend over Italy from 1961 to 2004. Theor Appl Climatol 91:51–58

Tshiala MF, Olwoch JM, Engelbrecht FA (2011) Analysis of temperature trends over Limpopo province, South Africa. J Geogr Geol 3:13–21

Turkes M, Sumer UM, Kilic G (1996) Observed changes in maximum and minimum temperatures in Turkey. Int J Climatol 16:436–477

Unganai LS (1996) Historic and future climatic change in Zimbabwe. Clim Res 6:137–145

Urquhart P (2008) IFAD's response to climate change through support to adaptation and related actions. In: Comprehensive report: final version, p 160

van Regenmortel G (1995) About global warming and Botswana temperatures. Botsw Notes Rec 27:239–255

Vives B, Jones RN (2005) Detection of abrupt changes in Australian decadal rainfall (1890–1989). In: Technical paper no. 73, pp 1–54. CSIRO Marine and Atmospheric Research, Hobart

Von Neumann J (1941) Distribution of the ratio of the mean square successive difference to the variance. Ann Math Stat 13:367–395

Von Storch H (1995) Misuses of statistical analysis in climate research. In: Von Storch H, Navarra A (eds) Analysis of climate variability: applications of statistical techniques. Springer, Berlin

Vose RS, Easterling DR, Gleason B (2005) Maximum and minimum temperature trends for the globe: an update through 2004. Geophys Res Lett 32:L23822

Wang F, Zhang C, Peng Y, Zhou H (2014) Diurnal temperature range variation and its causes in a semiarid region from 1957 to 2006. Int J Climatol 34:343–354

Wolski P, Savenije HHG, Murray-Hudson M, Gumbricht T (2006) Modelling of the flooding in the Okavango Delta, Botswana, using a hybrid reservoir-GIS model. J Hydrol 331:58–72

Wu L, Zhang J, Dong W (2011) Vegetation effects on mean daily maximum and minimum surface air temperatures over China. Chin Sci Bull 56:900–905

Yadav RR, Park W, Singh J, Dubey B (2004) Do the western Himalayas defy global warming? Geophys Res Lett 31:L17201. doi:10.1029/2004GL020201

Yang T, Chen X, Xu CY, Zhang ZC (2009) Spatio-temporal changes of hydrological processes and underlying driving forces in Guizhou region, Southwest China. Stoch Environ Res Risk Assess 23:1071–1087

Yao W, Li L (2014) A new regression model: modal linear regression. Scand J Statist 41:656–671

Ye XC, Zhang Q, Liu J et al (2013) Distinguishing the relative impacts of climate change and human activities on variation of streamflow in the Poyang lake catchment, China. J Hydrol 494:830–895

Yonetani T (1993) Detection of long term trend, cyclic variation and step-like change by the Lepage test. J Meteorol Soc Jpn 71:415–418

Yue S, Pilon PJ, Phinney B, Cavadias G (2002) The influence of autocorrelation on the ability to detect trend in hydrological series. Hydrol Process 16:1807–1829

Zarenistanak M, Dhorde AG, Kripalani RH, Dhorde AA (2015) Trends and projections of temperature, precipitation, and snow cover during snow cover-observed period over southwestern Iran. Theor Appl Climatol 122:421–440

Zhou L, Dickinson RE, Tian Y, Vose RS, Dai Y (2007) Impact of vegetation removal and soil aridation on diurnal temperature range in a semiarid region: application to the Sahel. PNAS 104:17937–17942

Zhou L, Dai A, Dai Y, Vose RS, Zou C-Z, Tian Y, Chen H (2009) Spatial dependence of diurnal temperature range trends on precipitation from 1950 to 2004. Clim Dyn 32:429–440